Journal of Volcanology and Geothermal Research 285 (2014) 214–228

Contents lists available at ScienceDirect

Journal of Volcanology and Geothermal Research

journal homepage: www.elsevier.com/locate/jvolgeores

The geological and structural evolution of the Cerro Tuzgle Quaternary stratovolcano in the back-arc region of the Central Andes, Argentina

G. Norini [a,*], S. Cogliati [b], W. Baez [c], M. Arnosio [c], E. Bustos [c], J. Viramonte [c], G. Groppelli [a]

[a] *Istituto per la Dinamica dei Processi Ambientali—Sezione di Milano, Consiglio Nazionale delle Ricerche, Milano, Italy*
[b] *Dipartimento di Scienze dell'Ambiente e del Territorio e di Scienze della Terra, Università degli Studi di Milano-Bicocca, Milano, Italy*
[c] *Instituto Geonorte-INENCO, Universidad Nacional de Salta—CONICET, Salta, Argentina*

A R T I C L E I N F O

Article history:
Received 24 June 2014
Accepted 21 August 2014
Available online 29 August 2014

Keywords:
Synthemic units
Volcanotectonic interplay
Geological map
Sector collapse

A B S T R A C T

The aim of our paper is to contribute to a better knowledge of the volcanism in the back-arc region of the Central Andes and its relationships with the basement geology, the stress field and the tectonic evolution, by studying in detail the stratigraphy and the structure of the Quaternary Cerro Tuzgle stratovolcano in the Puna Plateau. Field mapping and remote sensing analysis reveal the stratigraphic architecture, the geological evolution and the volcanotectonic interactions in the Cerro Tuzgle area. For the first time in a volcano of the Puna Plateau, synthemic units bounded by unconformity surfaces have been defined, unrevealing the temporal and spatial relationships between constructive and destructive phases of the volcano history. Our study indicates that after the emplacement of a small ignimbrite deposit and of few scattered lava domes, the central Cerro Tuzgle volcano built up throughout three distinct phases of edifice construction. The first of these constructive phases ended with a previously unreported destructive event, consisting of ≈0.5 km^3, catastrophic sector collapse of the volcanic edifice, whose stratigraphic position and main characteristics have been identified. The study suggests that the regional stress regime and the topography of the substrata are the main non-magmatic factors controlling the constructive and destructive phases of the volcano, including the directions of magmatic intrusions, faulting and gravitational sector failure of the volcano. The integration of synthemic stratigraphy and volcanotectonic analysis in the study of volcanic edifices showed to be an effective methodological approach for the understanding of the magmatic and tectonic evolution of the Puna Plateau.

1. Introduction

During the last years much effort has been made in the understanding of the origin and evolution of the back-arc volcanism of the Puna Plateau in the Central Andes (Fig. 1). Along with regional studies on the petrochemical features of magmas and the tectonic, magmatic and stratigraphic characteristics of the back-arc area, few works have been focused on the evolution of single volcanic edifices, like monogenetic effusive and phreatomagmatic centres, stratovolcanoes and calderas (e.g. Viramonte et al., 1984; Salfity, 1985; Viramonte and Petrinovic, 1990; Coira and Kay, 1993; Riller et al., 2001; Matteini et al., 2002; Petrinovic et al., 2005; Ramelow et al., 2006; Guzmán et al., 2006; Petrinovic et al., 2006; Trumbull et al., 2006; Mazzuoli et al., 2008; Kay and Coira, 2009; Kay et al., 2010; Petrinovic et al., 2010; Acocella et al., 2011; Norini et al., 2013). Many of these works pointed out the strict relationship among the transport of magma to the surface, the evolution of the volcanic centres and the geometry and kinematics of the tectonic faults (e.g. Riller et al., 2001; Petrinovic et al., 2005; Ramelow et al., 2006; Petrinovic et al., 2006, 2010). Identifying the transport, emplacement and eruption mechanisms of the back-arc volcanoes and their interplay with the basement geology, stress field and tectonic structures have been shown to be crucial for the understanding of the magmatic and tectonic processes in the Central Andes (e.g. Acocella et al., 2011). A better knowledge of these mechanisms may also be very useful for the assessment of volcanic hazard and the exploration of geothermal reservoirs and ore deposits in the back-arc portions of convergent margins (e.g. Petrinovic et al., 2010; Giordano et al., 2013). Among the volcanic centres in the back-arc region of the Central Andes, many small to medium sized stratovolcanoes punctuate the Puna Plateau, like the Rincon, Chimpa, Quevar, El Azufre, Tul Tul, Del Medio, Pocitos and Cerro Tuzgle volcanoes, for which very few data have been published before (e.g. Acocella et al., 2011) (Fig. 2).

The aim of our paper is to contribute to a better knowledge of the volcanism in the back-arc region of the Central Andes, by studying in detail the stratigraphy, geological evolution and volcanotectonic processes of the youngest of the Puna Plateau polygenetic volcanic centres, the Quaternary Cerro Tuzgle stratovolcano (<0.65 Ma) (Coira and Kay, 1993) (Fig. 2). For this purpose we mapped with remote sensing and in the field all the volcaniclastic and lava units belonging to the Cerro Tuzgle volcano. We employed lithostratigraphic units as the main criterion for fieldwork and geological mapping. The recognition of unconformity

* Corresponding author. Tel.: +39 0266173334; fax: +39 0228311442.
E-mail address: gianluca.norini@cnr.it (G. Norini).

http://dx.doi.org/10.1016/j.jvolgeores.2014.08.023
0377-0273/

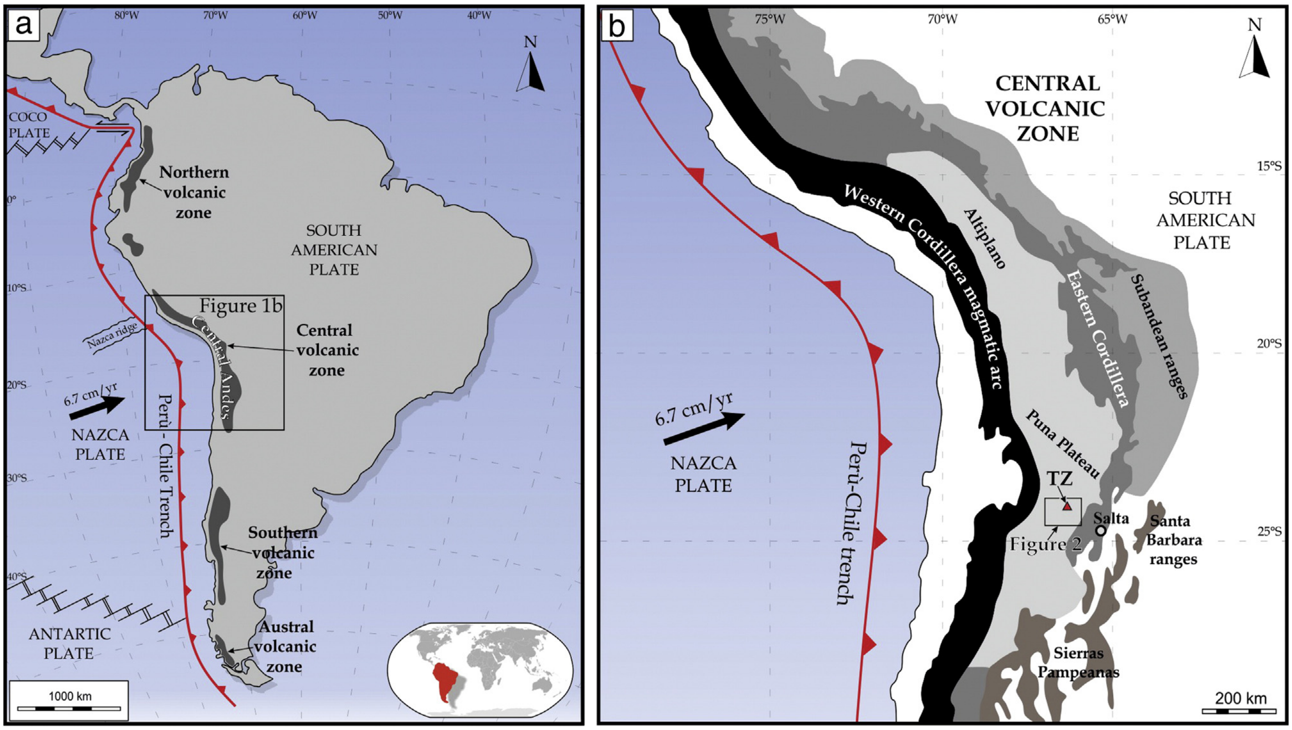

Fig. 1. a) Location of the Central Volcanic Zone in the geodynamic framework of South America; volcanic zones are depicted in dark grey. The location of Fig. 1b is also shown. b) Position of the Cerro Tuzgle volcano (TZ, depicted by a red triangle) in the regional framework of the Puna Plateau–Altiplano, the location of Fig. 2 is shown. (For interpretation of the references to colour in this figure legend, the reader is referred to the web version of this article.)

surfaces has enabled several lithostratigraphic units to be grouped in Unconformity Bounded Stratigraphic Units (UBSU, synthemic units). The adoption of the synthemic unit criteria allowed the synthesis of temporal and spatial relations among constructive and destructive phases of the volcano history, linking stratigraphic information together with morphogenetic and tectonic processes (e.g. Branca et al., 2004; Bellotti et al., 2006; Branca et al., 2011). We also focused our fieldwork on the volcanotectonic structure of the Tuzgle edifice, to identify the main deformation features and the interplay among the stress field, the basement faults and the volcanic activity. As a result of our study, we propose a new detailed geological map of the Cerro Tuzgle volcano and a reconstruction of its volcanic evolution in the geological and structural framework of the back-arc Puna Plateau.

2. Background: geological and structural setting of the Puna Plateau

The Central Andes comprises the vast back-arc Altiplano-Puna plateau, delimited by the Western Cordillera magmatic arc to the west and the Eastern Cordillera and Subandean Ranges to the east (Fig. 1b). The Puna Plateau is an internally drained plateau that constitutes the southern sector of the Altiplano–Puna region. Since the Eocene–Oligocene the Puna Plateau formed by crustal shortening and thickening, with both orogen-parallel thrusting and orogen-oblique strike-slip faulting (Allmendinger et al., 1983; Jordan et al., 1983; Salfity, 1985; Isacks, 1988; Dewey and Lamb, 1992; Allmendinger and Gubbels, 1996; de Urreiztieta et al., 1996; Allmendinger et al., 1997; Kley and Monaldi, 1998; Coutand et al., 2001; Riller et al., 2001; Riller and Oncken, 2003; Elger et al., 2005; Barnes and Ehlers, 2009; Norini et al., 2013). The far-field stress responsible for the crustal shortening regime is imparted by the plate convergence between the Nazca and South American plates (Gripp and Gordon, 1990; Assumpção, 1992; DeMets et al., 1994; Klotz et al., 1999; Norabuena et al., 1999; Ramos, 2009).

The Puna Plateau basement of Late Neoproterozoic to Cambrian age is represented by the Puncoviscana Formation, composed mainly of deformed meta-sedimentary rocks, and by the Mesón Group, made of siliciclastic sediments (Turner, 1960, 1964; Blasco et al., 1996; Sanchez and Salfity, 1999; Aceñolaza and Aceñolaza, 2005). The Precambrian and Cambrian units are intruded by the metagranitoid rocks of the Ordovician Faja Eruptiva, and are covered through a marked unconformity by an Ordovician volcano-sedimentary sequence (Coira, 1973; Mendez et al., 1973; Allmendinger et al., 1983; Blasco et al., 1996; Viramonte et al., 2007) (Fig. 2).

The Cretaceous–Paleocene sedimentary sequence of the Salta Group (Fig. 2) and the Oligocene–Miocene siliciclastic and evaporitic deposits of the Pozuelos Formation crop out above the Pre-Cambrian and Palaeozoic local basement (Turner, 1960, 1964; Schwab and Lippolt, 1976; Koukharsky and Munizga, 1990; Alonso, 1993; Blasco et al., 1996). The Salta Group was formed during an initial phase of rifting followed by a period of thermal subsidence, and is divided into three sub-groups (Pirgua, Balbuena, and Santa Barbara sub-groups), representing different stages in the evolution of the rift (Reyes and Salfity, 1973; Galliski and Viramonte, 1988; Salfity and Marquillas, 1994; Viramonte et al., 1999; Palma, 2000; Marquillas et al., 2005; Salfity and Monaldi, 2006; Monaldi et al., 2008).

The basins of the Salta Group and Pozuelos Formation were inverted during the subsequent orogenic phases started in the Eocene–Oligocene and leading to the uplift of the Puna Plateau (Salfity et al., 1993; Reynolds et al., 2000; Coutand et al., 2001; Kley and Monaldi, 2002; Carrapa et al., 2005; Hongn et al., 2007; Monaldi et al., 2008). The plateau has a basin-and-range morphology, with the N–S trending valleys filled by continental clastic sediments and volcanic rocks of Miocene–Quaternary age (e.g. Wigger et al., 1994; Beck et al., 1996; Blasco et al., 1996; Allmendinger et al., 1997; Kraemer et al., 1999; Coutand et al., 2001; Sobel et al., 2003; Carrapa et al., 2005; Coutand et al., 2006; Giordano et al., 2013; Norini et al., 2013) (Fig. 2). The structural style of the plateau is characterized by the Precambrian–Ordovician units thrusted over the Cretaceous–Recent sedimentary and volcanic rocks, with vertical strike-slip orogen-oblique faults developed as transfer structures connecting some of the listric orogen-parallel thrusts (Allmendinger et al., 1983; Cladouhos et al., 1994; Marrett et al., 1994;

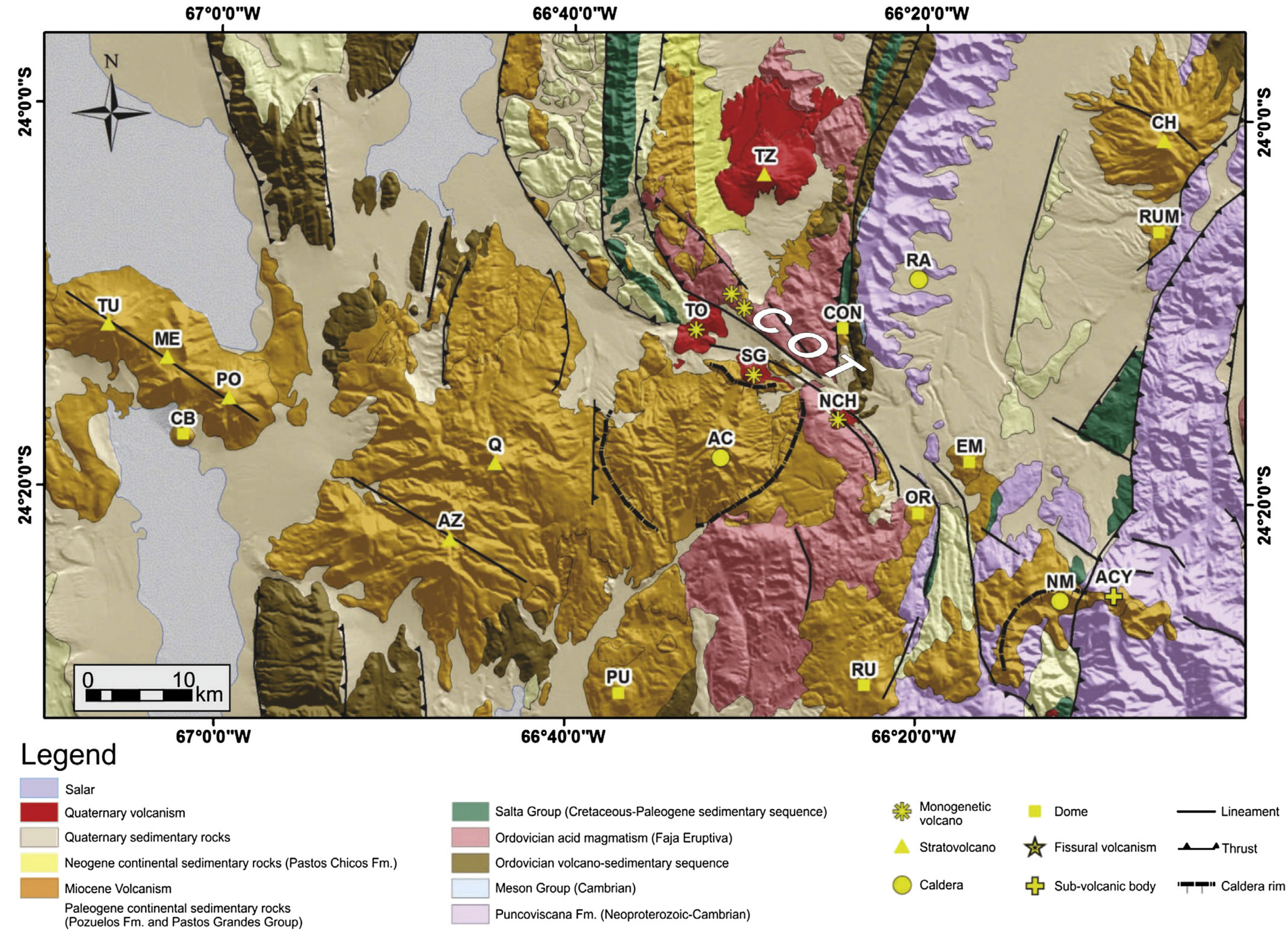

Fig. 2. Regional geological map of the back-arc Puna Plateau in the Cerro Tuzgle area on a SRTM shadow relief (partly modified from Blasco et al. (1996) and Norini et al. (2013)). TU: Tul Tul; ME: Del Medio; PO: Pocitos; CB: Cerro Bola; AZ: El Azufre; Q: Quevar; PU: Pucara; RU: Rupasca; AC: Aguas Calientes; OR: Organullo; NCH: Negro del Chorrillo; SG: San Geronimo; TO: Tocomar; TZ: Tuzgle; CON: Concordia; RA: Ramada; EM: El Morro; NM: Negra Muerta; ACY: Nevado de Acay; CH: Chimpa; RUM: Rumio; COT: Calama–Olacapato–El Toro Fault System.

Marrett and Strecker, 2000; Coutand et al., 2001; Omarini et al., 2001; Riller et al., 2001; Riller and Oncken, 2003; Norini et al., 2013).

2.1. Volcanism in the Puna Plateau

Volcanism in the Cenozoic Andean Cordillera is the product of subduction of the Nazca and Antarctica Plates beneath the South American Plate (Fig. 1a). Complex segmentation of the tectonic, magmatic and sedimentary processes through time and space defined distinct tectonomagmatic sectors within the cordillera (e.g. Coira et al., 1982; Stern, 2004; Ramos, 2009). In the Central Andes, Miocene–Quaternary volcanic activity occurred within the Central Volcanic Zone in two well-defined segments: the Western Cordillera magmatic arc and the Altiplano–Puna Plateau back-arc region (Fig. 1b). The occurrence of extensive volcanic activity in the Puna Plateau has been attributed to NW–SE, vertical, strike-slip faults, tapping mid-crustal magma sheets originated by slab steepening or delamination of the thickened lower crust and mantle lithosphere (e.g. Allmendinger et al., 1983; Salfity, 1985; Yuan et al., 2000; Riller et al., 2001; Matteini et al., 2002; ANCORP Working Group, 2003; Petrinovic et al., 2006; Trumbull et al., 2006; Kay and Coira, 2009; Acocella et al., 2011). Also, a role played by the orogen-parallel thrust faults in focusing hydrofractures arrest, magma chamber formation and the emplacement of polygenetic volcanoes has been recently proposed by Norini et al. (2013). The best exposed NW–SE tectonic structure in the Puna Plateau is the Calama–Olacapato–El Toro (COT) fault system, an active left-lateral strike-slip fault zone associated with several Miocene to Quaternary volcanoes, comprising the Cerro Tuzgle stratovolcano (Fig. 2) (e.g. Allmendinger et al., 1983; Viramonte et al., 1984; Salfity, 1985; Matteini et al., 2002; Ramelow et al., 2006; Petrinovic et al., 2006; Mazzuoli et al., 2008; Acocella et al., 2011; Norini et al., 2013).

In the Cerro Tuzgle area, in the back-arc region, two different eruptive cycles have been identified based on radiometric age of the magmatic products. The first cycle took place between 17.15 and 5.3 Ma and interested all the sectors of the plateau, the second cycle dates back to the Quaternary (<1.5 Ma) and only interested the central-eastern part of the Puna Plateau (Coira and Kay, 1993; Trumbull et al., 2006; Mazzuoli et al., 2008; Petrinovic et al., 2010; Acocella et al., 2011 and references therein). In the first magmatic cycle (17.15–5.3 Ma), volcanic centres consist mainly of basaltic–dacitic stratovolcanoes (Rincon, Tul-Tul, Del Medio, Pocitos, Quevar, Azufrero and Chimpa), andesitic–rhyolitic calderas (Aguas Calientes, Negra Muerta), rhyolitic phreatomagmatic vents (Ramadas) and dacitic domes (El Morro, Organullo, Rupasca and Concordia) (Acocella et al., 2011, and references therein) (Fig. 2).

After the deposition of the Upper Miocene–Pliocene sedimentary clastic succession of continental conglomerates, sandstones and siltstones of the Pastos Chicos Formation (Giordano et al., 2013), magmatic activity resumed in the central Puna Plateau with the emplacement of small rhyolitic ignimbrite blankets (Tuzgle ignimbrites), rhyolitic phreatomagmatic pyroclastic deposits (Tocomar), shoshonitic monogenetic scoria cones/effusive basalts (Negro de Chorrillos and San

Jeronimo), and the polygenetic Cerro Tuzgle volcano (Acocella et al., 2011, and references therein) (Fig. 2).

2.2. The Cerro Tuzgle volcano

The Quaternary Cerro Tuzgle stratovolcano (0.65 Ma—Holocene?, Schwab and Lippolt, 1976; de Silva and Francis, 1991; González-Ferrán, 1995) is one of the most prominent volcanic edifices within the back-arc Andes. It is located about 280 km behind the active magmatic arc and belongs to the Miocene–Quaternary volcanic sequence of the Puna Plateau. The Cerro Tuzgle is a high-K calcalkaline andesitic-rhyodacitic volcanic centre with an altitude of 5486 m a.s.l. (Coira and Kay, 1993). The volcano is located in a N-S-trending, thrust faults-bounded, intramontane depression. This tectonic depression is closed by the main COT fault scarps 10–15 km south of the Cerro Tuzgle, and has a northward gently dipping floor, from 4400 m a.s.l. to the south of the stratovolcano to 4100 m a.s.l. to the north of it (Norini et al., 2013, and references therein) (Fig. 2).

The volcanic activity of the Cerro Tuzgle has been fed by a mid-crustal magma sheet located below the Puna Plateau (Cahill et al., 1992; Coira and Kay, 1993; Yuan et al., 2000; Riller et al., 2001). A zone of magma ponding between 8 and 22 km of depth, just above the mid-crustal magma sheet, has been imaged by magnetotelluric and gravimetric surveys (Mon, 1987; Sainato and Pomposiello, 1997). Coira and Kay (1993) reported thermobarometric data suggesting a >2.5 to 3 kbar pre-eruption crystallization pressure for the oldest unit of the Cerro Tuzgle volcanic succession, the Tuzgle Ignimbrite, and a 5–6 kbar pre-eruption crystallization pressure for the overlying lava units. With a lithostatic pressure gradient of 0.26–0.28 kbar/km, the crystallization pressures correspond to depths of about 10–20 km below the surface (Zang and Stephansson, 2010). These depths have been considered consistent with ponding and evolution of Cerro Tuzgle magmas beneath the sole of the main N–S-striking thrust faults, representing mechanical barriers for hydrofractures arrest and magma chambers formation (Coira and Kay, 1993; Norini et al., 2013).

Coira and Kay (1993) recognize 6 main phases of Cerro Tuzgle volcanic activity, beginning with a wide plateau made of rhyodacitic pyroclastic flow deposits (Tuzgle Ignimbrite, 0.65 $\pm$ 0.18 Ma, Schwab and Lippolt, 1976), followed by a dacitic lava dome complex located along the caldera rim of the Tuzgle Ignimbrite (Old Complex Unit, 3.5 km^3), by andesitic lava flows (Pre-platform Unit, 0.3 $\pm$ 1.0 Ma, Aquater, 1980), and by prominent mafic andesitic lava flows (Platform Unit). A tectonic event characterized by vertical faults, E–W and NW–SE oriented, dissected the older units and fed the younger Post-platform Unit and the latitic Young Flow Unit (Coira and Paris, 1981). Even if the Young Flow Unit has been dated at 0.1 $\pm$ 0.1 and 0.1 $\pm$ 0.3 Ma (Schwab and Lippolt, 1976), it is supposed to be of Holocene age (de Silva and Francis, 1991; González-Ferrán, 1995) or at the Pleistocene–Holocene boundary (Coira and Kay, 1993). Pre-platform, Platform, Post-platform and Young Flow units present a total volume of about 0.5 km^3 and form the central volcanic edifice (Coira and Kay, 1993).

3. Stratigraphy and geological mapping of the Cerro Tuzgle volcano

The study of the Cerro Tuzgle geology began with the analysis of digital elevation models (DEMs), orthorectified satellite imagery and aerial photographs, plus a critical recompilation of the geological map of Coira and Kay (1993). The morphology and boundaries of the main volcanic units and structures have been mapped in a Geographic Information System (GIS) from Aster satellite images (channels 1, 2, 3 with resolution of 15 m) (Pieri and Abrams, 2004); B/W aerial photographs at 1:50,000 scale; shaded relief images of DEMs computed from SRTM data (90 m resolution) (USGS, 2006) and digital photogrammetry of the aerial photographs (10 m resolution).

The exceptional exposure and lack of vegetated land in the high-altitude hyperarid Puna region allowed comprehensive and precise remote mapping of many of the lava flows and volcaniclastic units cropping out on the volcano flanks. Most of these units have been then verified in the field through the analysis of 69 accessible outcrops (Fig. 3). The fieldwork was conducted at the 1:10,000 scale and based on contour maps derived from the DEMs and orthorectified satellite images, due to the lack of published topographic maps at a reasonable scale. The resulting geological map at the 1:25,000 scale covers an area of 180 km^2 (presented with synthemic units at the 1:70.000 scale in Fig. 4). Description of the lithology and stratigraphic relationships were conducted on all the visited outcrops. The petrographic characteristics of the outcropping units have also been described in thin sections, mainly to support correlations among clastic deposits and lavas.

The volcanic units visited in outcrops are well preserved lava flows and volcaniclastic deposits. Unconformity surfaces consisting of angular unconformities and erosive non conformities have been identified among these units, and interpreted as the record of main episodes of change in volcanic activity, erosional events and volcanotectonic deformations, as the volcano construction progressed during time (Fig. 5).

3.1. Stratigraphic succession and main unconformities of the Cerro Tuzgle volcano

At the base of the stratigraphic succession of the Cerro Tuzgle volcano, metagranitoid and volcano-sedimentary Ordovician rocks crop out on the eastern side of the mapped area (Blasco et al., 1996) (Fig. 4). The Ordovician units are covered by the Miocene dacitic ignimbrite deposit of the Trinchera Formation and by the Upper Miocene–Pliocene sedimentary succession of the Pastos Chicos Formation, to the south and west of the mapped area, respectively (Petrinovic et al., 2010; Giordano et al., 2013) (Figs. 4 and 6).

After the deposition of the continental clastic sediments comprised in the Pastos Chicos Formation, a local non conformity marks a temporal hiatus (from >2.5 Ma to 0.65 Ma, Schwab and Lippolt, 1976; Giordano et al., 2013) and the subsequent resume of volcanic activity in the central Puna Plateau.

In the stratigraphy of the Cerro Tuzgle volcano a generally homogeneous lithology characterizes each synthem, allowing to correlate and to group the different lithostratigraphic units and, at the same time, to describe their petrographic and geochemical composition on the base of the synthemic classification (Table 1).

3.1.1. Tuzgle Ignimbrite Synthem

The stratigraphic sequence of the Cerro Tuzgle volcano starts with the 0.5 km^3 Tuzgle Ignimbrite (e.g. Coira and Kay, 1993). This pyroclastic flow deposit, dated at 0.65 $\pm$ 0.18 Ma (Schwab and Lippolt, 1976), creates a wide 80 m-thick plateau to the north and north-west of Cerro Tuzgle (Fig. 4). The Tuzgle Ignimbrite is homogeneous throughout its extension, shows light yellow–white colour, has vertical columnar joints and is moderately indurated by vapour phase crystallization in its upper part (outcrop Tzg03 of Figs. 3, 7). The deposit is massive, pumice-rich (30–35%), matrix supported, with slight reverse grading of rounded juvenile pumices (up to 6 cm) and normal grading of angular lithic fragments made of metamorphic, plutonic and volcanic rocks (up to 5 cm). Matrix is crystal-rich fine ash made of plagioclase, quartz, biotite, sanidine, orthopyroxene, zircon and oxides. Pumices in thin section are described in Table 1.

Even if the emission vent of this pyroclastic deposit has not been identified, its limited extension, following the gently northward dipping pre-volcano topography, suggests that it originated form a buried structure (small collapse caldera) centred beneath the present Cerro Tuzgle edifice (Coira and Kay, 1993).

At the top of the Tuzgle Ignimbrite, an evident angular unconformity with the overlying lithostratigraphic units marks a change in eruptive style, from explosive activity to effusive volcanic products (Fig. 5a).

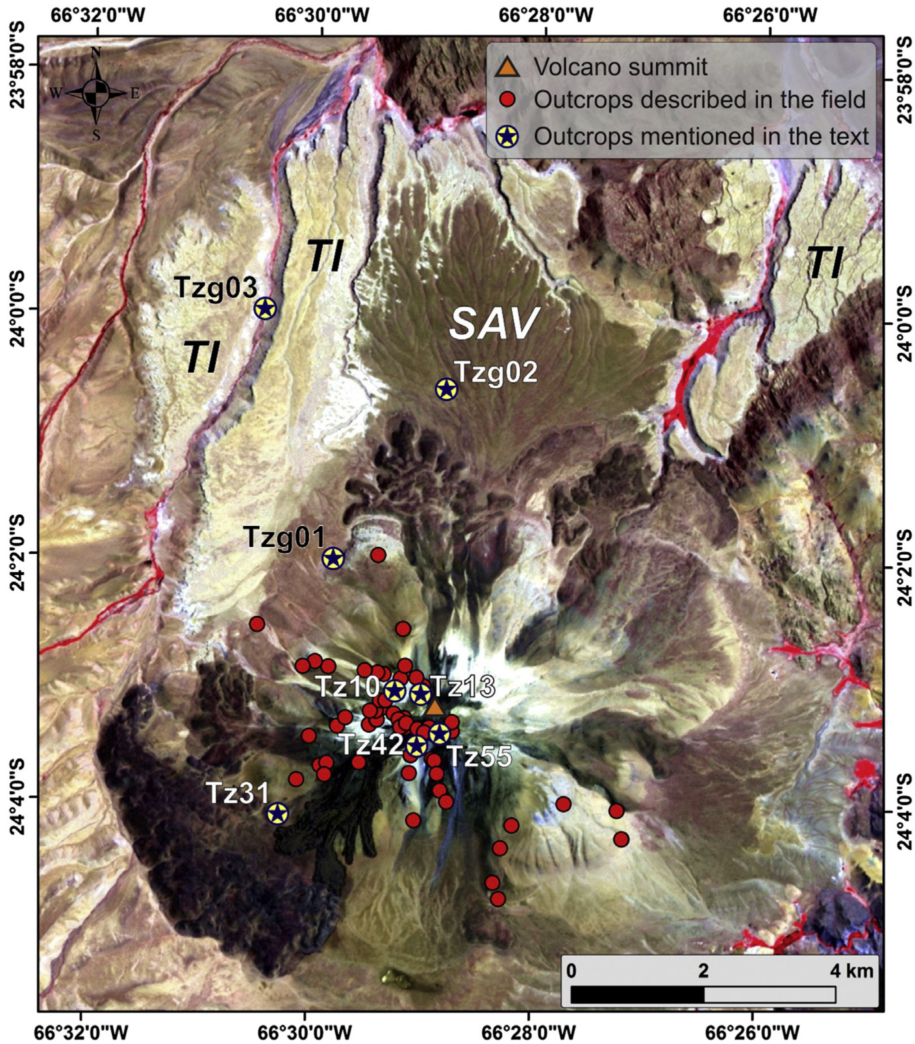

Fig. 3. Location of the outcrops described in the field and mentioned in the text on an Aster satellite image of the fieldwork area (channels 1, 2, 3 with resolution of 15 m). SAV: San Antonio Volcaniclastic unit, depicted in shades of brown. TI: Tuzgle Ignimbrite unit, depicted in shades of light yellow–light brown. (For interpretation of the references to colour in this figure legend, the reader is referred to the web version of this article.)

3.1.2. Basal Dome Complex Synthem

A series of six lithostratigraphic units corresponding to lava domes have been mapped along the periphery of Cerro Tuzgle, in the south-eastern, eastern and northern sectors of the volcano (Fig. 4). These circular and flat-topped domes are formed by homogeneous lava deposits, light grey to brown-reddish in colour, with maximum observed thickness of 50 meters (outcrop Tzg01 of Fig. 3). Complex flow structures and laminations are common in all outcrops (Fig. 8). The lavas have a porphyritic and thinly-vesiculated to non-vesiculated texture, with <20 cm rounded magmatic xenoliths (Table 1). The wide spatial distribution of the lava domes around the volcano periphery and their well constrained stratigraphic position suggest a magmatic phase of viscous lava emplacement, representing the emplacement of a lava domes complex with a not well defined eruptive axis (Coira and Kay, 1993). The spatial distribution of some lava domes, arranged in a semicircle, could be controlled by the ring faults and other structures associated with the caldera collapse of the Tuzgle Ignimbrite.

At the top of these lava domes, an angular unconformity with the overlying lithostratigraphic units marks the establishment of a central feeding system and a change of the eruptive style toward less viscous effusive products (Fig. 5b).

3.1.3. San Antonio Synthem

Six lithostratigraphic units corresponding to lava flows radiating from a common emission area have been defined and mapped on the north-western and southern flanks of Cerro Tuzgle (Fig. 4). These lava flows are massive, dark grey to brown-reddish in colour, with maximum observed thickness of 30 m (outcrop Tz10 of Figs. 3, 9). The lavas generally have a porphyritic and slightly-vesiculated texture, are rich in mega-xenocrystals of plagioclase (<10 cm), with abundant large (<40 cm) rounded magmatic xenoliths (Coira and Kay, 1993) (Table 1). Attitude data show that these lavas flowed on slopes of more than 15°–20°, suggesting that a steep central volcanic cone was already established when they have been emplaced, and then representing the first recognized constructive event of the Cerro Tuzgle central volcano.

At the northern base of the central volcano, a well exposed volcaniclastic fan with a surface of 12 km^2 has been mapped. This fan is homogeneous in satellite views and composed of a single volcaniclastic deposit, the San Antonio Volcaniclastic (SAV) unit, with an estimated thickness of at least 30–40 m (Figs. 3 and 9d). The SAV overlies the Tuzgle Ignimbrite unit (*Tuzgle Ignimbrite Synthem*) and is covered and sealed upslope by a lava flow of the younger *Azufre Central Volcano*

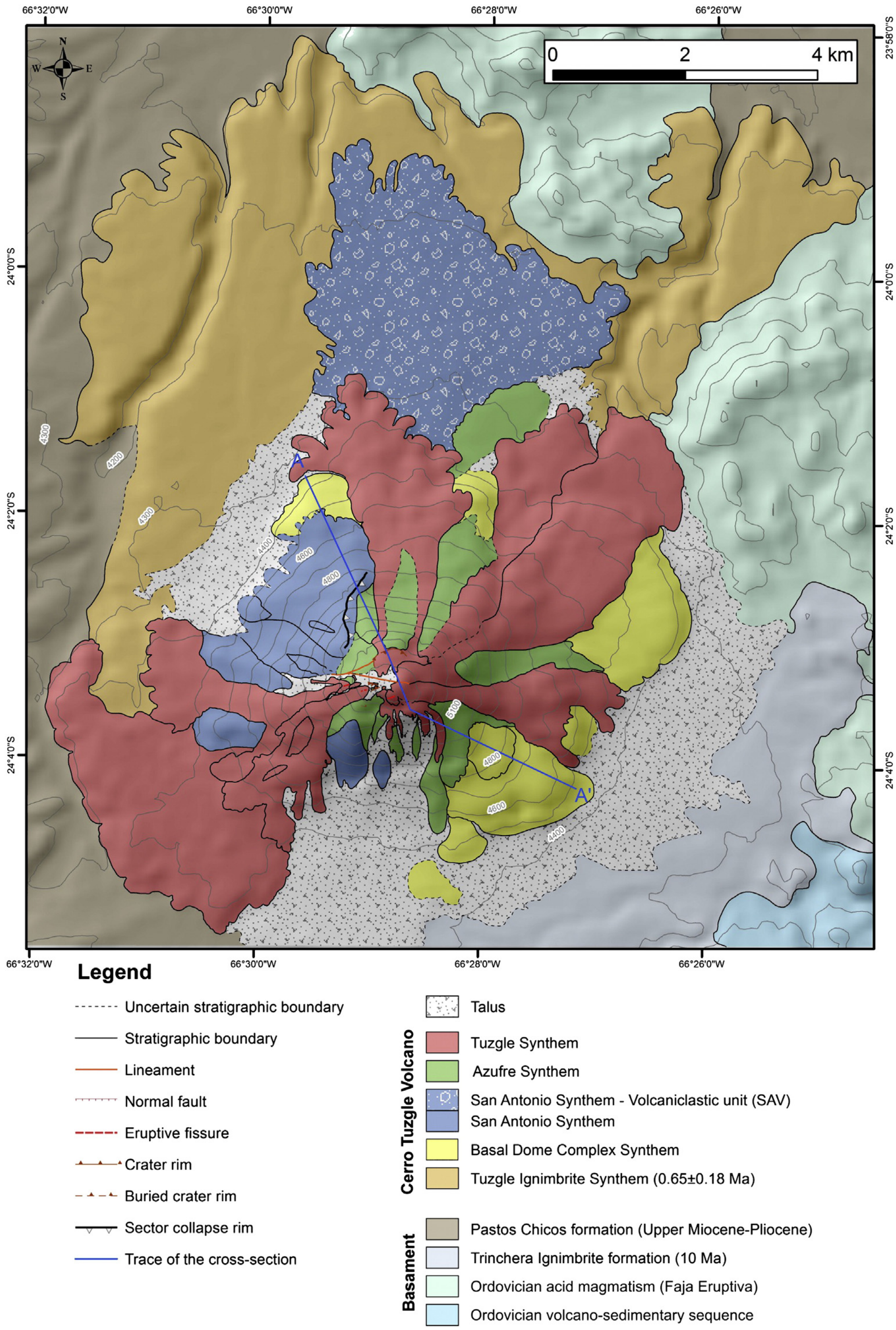

Fig. 4. Geological map of the Cerro Tuzgle volcano based on the synthemic units. The trace of the schematic geological cross section A–A′ of Fig. 6 is shown.

Synthem (Section 3.1.4). In the field, the SAV deposit has a flat surface without clear evidences of hummocky morphology (Fig. 9d). No good sections of this deposit have been found in outcrop, where the SAV unit looks massive, matrix-supported, with unconsolidated sandy matrix and rounded monolithologic lava clasts up to 6–7 m in diameter (outcrop Tzg02 of Fig. 3). The clasts have a slightly-vesiculated texture, with porphyritic index of 20%–35%, and are rich in mega-xenocrystals of plagioclase (<10 cm) and large rounded magmatic xenoliths (<40 cm). The mineral association of clasts observed in thin section and their mega-xenocrystals and xenoliths contents are similar to those of the *San Antonio Synthem* lava flows. Even if the SAV unit is not clearly exposed and its base is not visible, its well-constrained spatial location, size and main internal features (massive, homogenous and monolithologic character) suggest that it was generated by a catastrophic en-mass failure of a significant portion of the central volcano.

At the top of the *San Antonio Synthem*, a sharp angular unconformity with the overlying lithostratigraphic units marks a major, previously unrecognized, volcanotectonic and erosive event (Section 4) (Fig. 5a, c, d). This event occurred before the construction of the central volcano resumed with new lava flows.

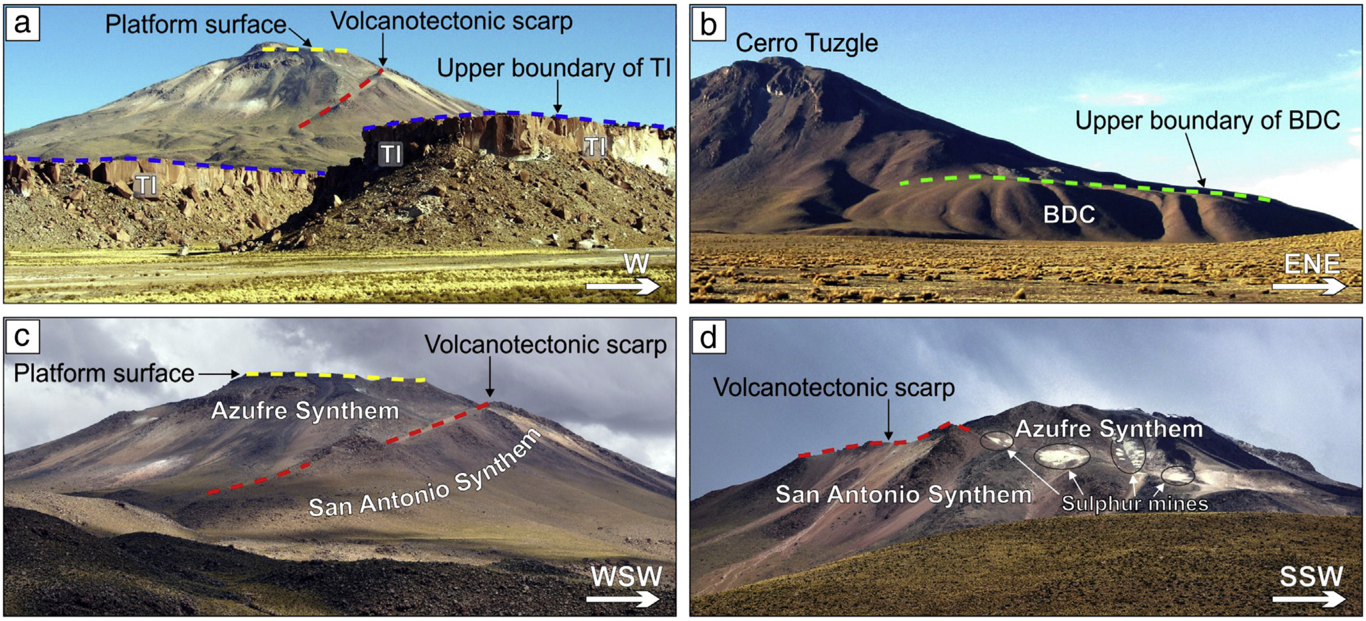

Fig. 5. Field photographs of Cerro Tuzgle depicting the main unconformities recognized in the volcano stratigraphy. a) View from north to south. b) View from SSE to NNW. c) View from NNW to SSE. d) View from WNW to ESE, location of the main sulphur mines on the western flank of the volcano is shown. Dashed line in blue depicts the angular unconformity at the top of the *Tuzgle Ignimbrite Synthem* (TI). Dashed line in green depicts the angular unconformity at the top of the *Basal Dome Complex Synthem* (BDC). Dashed line in red depicts the volcanotectonic scarp and angular unconformity at the top of the *San Antonio Synthem*. Dashed line in yellow depicts the angular unconformity named *Platform surface* at the top of the *Azufre Synthem*. (For interpretation of the references to colour in this figure legend, the reader is referred to the web version of this article.)

3.1.4. Azufre Synthem

A succession of nine lithostratigraphic units corresponding to lava flows radiating from a common emission point, coincident with the summit of Cerro Tuzgle, has been mapped on the volcano flanks (Fig. 4). The lava flows are massive, grey to brown-reddish in colour, with maximum observed thickness of 15 m (outcrop Tz13 of Figs. 3, 10). Some portions of the lava flows have a strong hydrothermal alteration, with sulphur precipitates and small abandoned mines for sulphur extraction on the southern, western and northern flanks of the volcano (Figs. 5c,d and 9b). The lavas generally have a porphyritic and slightly-vesiculated texture, seldom with mega-xenocrystals of plagioclase (<10 cm) and rounded magmatic xenoliths up to 20–30 cm in size (Table 1). On the whole, these lava flows correspond to the effusive volcanic activity occurred after the volcanotectonic event recognized at their base (Section 4), and then representing the second mapped constructive event of the central volcano in the stratigraphic record of Cerro Tuzgle.

At the top of these lava flows, an angular unconformity with the overlying lithostratigraphic units marks a volcanotectonic event, generating the flat 0.5 km^2 *Platform* surface near the volcano summit (Fig. 5a,c) (Coira and Kay, 1993).

3.1.5. Tuzgle Synthem

A series of 13 lithostratigraphic units corresponding to well preserved lava flows radiating from the volcano summit have been mapped on the flanks of Cerro Tuzgle (Fig. 4). These "aa" and block lava flows are black to grey in colour, with maximum observed thickness of 30 m (outcrop Tz31 in Figs. 3, 11). The lavas have a porphyritic and vesiculated texture (Table 1).

These lava flows correspond to the last eruptive activity recognized in the volcano stratigraphy, representing the third and final constructive event of the Cerro Tuzgle central volcano. Wide portions of the volcanic units of Cerro Tuzgle are partly covered by recent alluvial, colluvial and aeolian deposits (Fig. 4).

4. Volcanotectonic structures of Cerro Tuzgle

The main prominent structural features in the Cerro Tuzgle area are the orogen-parallel thrust faults and the orogen-oblique strike-slip faults, which have been extensively described in previous works (e.g. Norini et al., 2013, and references therein). These tectonic structures

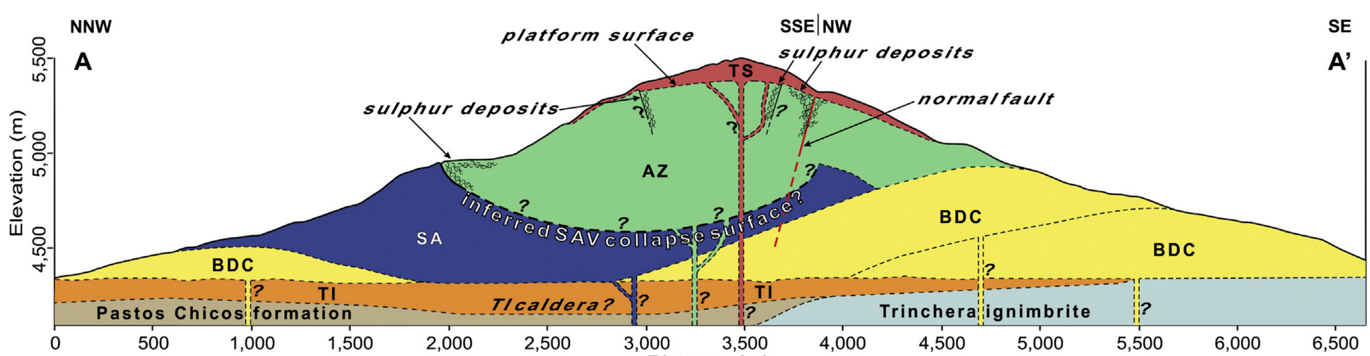

Fig. 6. Schematic geological cross section across the Cerro Tuzgle volcano. TI: Tuzgle Ignimbrite Synthem; BDC: Basal Dome Complex Synthem; SA: San Antonio Synthem; AZ: Azufre Synthem; TS: Tuzgle Synthem; SAV: San Antonio Volcaniclastic unit. The trace of the cross section is shown in Fig. 4. Legend as in Fig. 4.

Table 1
Schematic resume of the main lithologic, petrographic and geochemical characteristics of the Cerro Tuzgle volcanic products based on the synthemic classification.

Synthemic unit	Lithology	Texture	Structure	P.I.	Mineral association	Groundmass	Composition	Note
Tuzgle Ignimbrite Synthem	Pumice clasts, lithics fragments, glass shards and fragmented crystals	Pyroclastic texture	Pumice clasts with elongated to spherical vesicles	~10% (pumice)	Plagioclase (<1 cm), quartz (<1 cm), biotite (<3 mm), sanidine (<0.5 mm) (pumice)	Glassy matrix (pumice)	Rhyodacitic	Fig. 7b
Basal Dome Complex Synthem	Lava	Porphyritic texture	Perlitic fractures and spherulites. Iso-orientation of the microphenocrysts of sanidine and biotite parallel to the rim of the biggest phenocrystals	25–35%	Plagioclase (<3 cm), biotite (<2 mm), quartz (<4 mm), sanidine clinopyroxene (<0.4 mm), orthopyroxene (<1.5 mm), zircon (<0.1 mm) and oxides (<0.1 mm)	Glassy	Dacitic	Fig. 8b
San Antonio Synthem	Lava	Seriate flux texture	Iso-orientation of the microcrystals of biotite parallel to the rim of the biggest xenocrystals of plagioclase	15–35%	Plagioclase (<2 cm), biotite (<4 mm), quartz (<8 mm), orthopyroxene (<0.7 mm), clinopyroxene (<0.4 mm), Ti-amphibole (<0.4 mm), zircon (<0.1 mm) and oxides (<0.1 mm)	Glassy with microcrystals of oxides associate with biotite and plagioclase. Olivine, sanidine and orthopyroxene are also present as micro-xenocrystals and as glomerocrystals (<0.2 mm)	Andesitic–dacitic	Fig. 9c
Azufre Synthem	Lava	Seriate flux texture		25–35%	Plagioclase (<3 cm), biotite (<3 mm), quartz (<1 cm), Ti-amphibole (<1.5 mm), orthopyroxene (<1 mm), clinopyroxene (<1 mm), zircon (<0.1 mm) and oxides (<0.1 mm)	Glassy with spherulites	Andesitic–dacitic	Plagioclase sometimes has rims with sieve texture. Reaction crowns are present around the borders of some quartz crystals. Glomerocrystals of plagioclase, sanidine, orthopyroxene, clinopyroxene and amphibole have also been observed.Fig. 10b
Tuzgle Synthem	Lava	Seriate flux texture		25–35%	Plagioclase (4.9 mm), xenocrystals of quartz (3.9 mm), Ti-amphibole (1 mm), orthopyroxene (1.4 mm), clinopyroxene (1.2 mm), olivine (1.1 mm) and biotite (1.5 mm)	Vitreous	Andesitic	Coronitic rims of clinopyroxene around quartz xenocrystals and glomerocrystals of orthopyroxene, sanidine and plagioclase have been observed. Fig. 11b

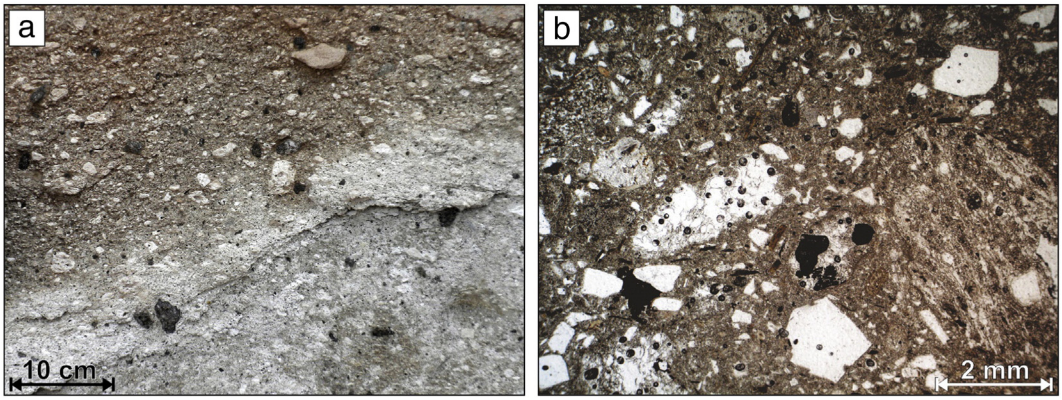

Fig. 7. *Tuzgle Ignimbrite Synthem*. Field photograph (a) and thin section (b) of the Tuzgle Ignimbrite deposit in outcrop TZG03. For location see Fig. 3.

run at the borders of the tectonic depression where the volcano is located and do not intersect the volcanic edifice at the surface (Fig. 2).

Associated with the main regional structures, the volcanic edifice exhibits volcanotectonic features, like (1) a prominent volcanotectonic scarp, (2) faults exposed in outcrop, and (3) eruptive fissures. All these recognized structural features related to the Cerro Tuzgle volcano were mapped and surveyed in the field. They have been used in this work for the interpretation of the volcanotectonic evolution of Cerro Tuzgle, and their descriptions are reported below.

4.1. Volcanotectonic scarp and relationship with the volcano stratigraphy

On the north-western flank of Cerro Tuzgle a prominent rectilinear scarp is exposed (Figs. 5a,c,d and 9b). This structural feature represents the main evidence of the angular unconformity at the boundary between the *San Antonio Synthem* and the *Azufre Synthem* (Section 3.1). This previously unreported scarp follows a general NNE–SSW trend and is continuous for 1.25 km across the volcanic edifice. The apparent lack of surface continuity of the scarp beyond the central volcano into the basement and the sharp decrease of the scarp height toward the volcano periphery indicate that it is a local volcanotectonic structural feature. Massive, thick lava flows of the *San Antonio Synthem* are cut upslope by the scarp, forming a sharp, 15–20 m-high counterslope on the otherwise uniform volcano flank (Figs. 9b and 12). This configuration indicates that the emission area of the lava flows of the *San Antonio Synthem* has been displaced/removed by the volcanotectonic event that generated the scarp, before it was sealed by the lava flows of the *Azufre Synthem*. The stratigraphic position of the scarp surface, in between two well defined synthems composed of lava flows emitted by a central volcano, suggests that it was formed suddenly by a catastrophic event (e.g. sector collapse), rather than gradually during the growth of the volcano.

4.2. Faults exposed in outcrops

The surface of the Cerro Tuzgle volcano is almost entirely made of recent fractured lava flows and unconsolidated coarse colluvial deposits, which mask most of the possible evidences of tectonic or volcanotectonic deformation. Despite extensive search, only on the upper southern flank of the cone, in outcrop Tz42, faults in a lava flow of the *Azufre Synthem* have been recognized (Figs. 3, 14 and 15). The outcrop is located in an abandoned sulphur mine, with the fault planes and fault zones showing white–yellow sulphur incrustations and some 2–4 mm-thick crystalline sulphur veins (Fig. 13). No slickenlines were measured, although there are displaced (10–20 cm) flow units in the lava deposit, indicating a normal component of motion on the fault planes. The measured faults and veins show a mean WNW–ESE orientation and have a dip angle ranging from 54° to 85° (Fig. 14).

4.3. Eruptive fissures

Field analysis of the youngest and best exposed lava flow of the *Tuzgle Synthem* (TZ lava flow) reveals that it was generated by three parallel eruptive fissures (Fig. 15). These features were mapped and measured because their orientation reflects the geometry of the magma feeding system, which is strictly connected to the regional and local stress field (Nakamura, 1977; Fink and Pollard, 1983; Tibaldi, 1995; Pasquaré and Tibaldi, 2003; Norini et al., 2006, 2010).

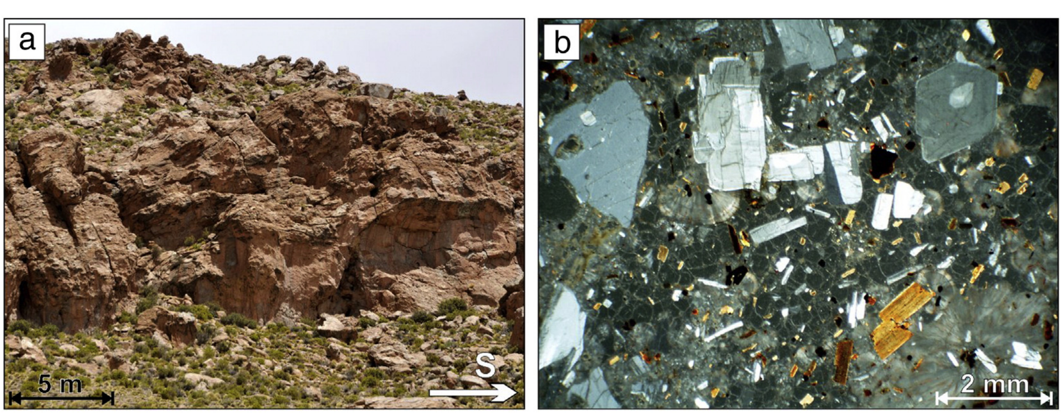

Fig. 8. *Basal Dome Complex Synthem*. Field photograph (a) and thin section (b) of the lava dome in outcrop TZG01. For location see Fig. 3.

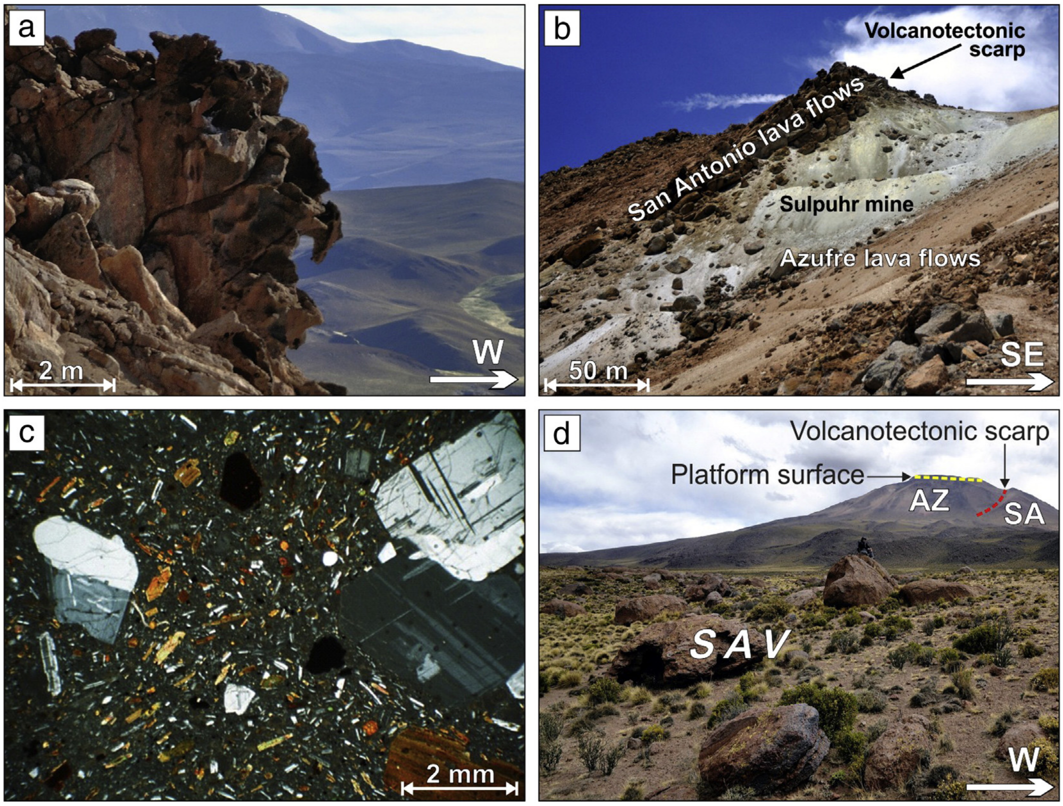

Fig. 9. *San Antonio Synthem*. Field photographs of a lava flow (a) and of the volcanotectonic scarp cutting upslope the lava flows of the San Antonio Synthem (b) in outcrop TZ10. c) Thin section of a lava flow sample collected in outcrop TZ10. d) Field photograph of the SAV deposit in outcrop TZG02. Dashed line in red depicts the volcanotectonic scarp and angular unconformity at the top of the *San Antonio Synthem* (SA); dashed line in yellow depicts the angular unconformity named *Platform surface* at the top of the *Azufre Synthem* (AZ). For location see Fig. 3. (For interpretation of the references to colour in this figure legend, the reader is referred to the web version of this article.)

The eruptive fissures are represented by elongated depressions and extensional fractures trending N80°E, bordered by rectilinear ridges 1–2 m high made of superimposed welded scoria deposits. Also, the easternmost eruptive fissure is exposed in a section, with several sub-vertical flow structures parallel to the general trend of the identified eruptive fissures (outcrop Tz55 in Figs. 3 and 15). The three fissures are aligned N110°E and are elongated N80°E, showing a right-stepping *en-echelon* arrangement (Fig. 15).

5. Discussion

The geological mapping and the stratigraphic data of the Cerro Tuzgle volcano, essentially based on synthemic units, allow the description of the volcanic evolution, relating the stratigraphic information with an effective synthesis of the major volcanic and volcanotectonic events, as discussed below.

In agreement with Coira and Kay (1993), the Quaternary volcanic activity in the Cerro Tuzgle area started with an ignimbritic eruption (0.65 ± 0.18 Ma, Schwab and Lippolt, 1976), whose source vent is buried under the central volcanic edifice. The ignimbrite flowed toward the north, following the gently northward dipping topography of the basement and the lateral constraint of the orogen-parallel ranges (Fig. 4). The pyroclastic deposit generated by this explosive eruption has been included in the *Tuzgle Ignimbrite Synthem*, limited at its base by a non conformity representing the resume of volcanic activity in the Puna Plateau, and at its top by an angular unconformity representing a significant change in volcanic activity.

After the ignimbritic eruption of the *Tuzgle Ignimbrite Synthem*, a change in eruptive style occurred, with the emplacement of the

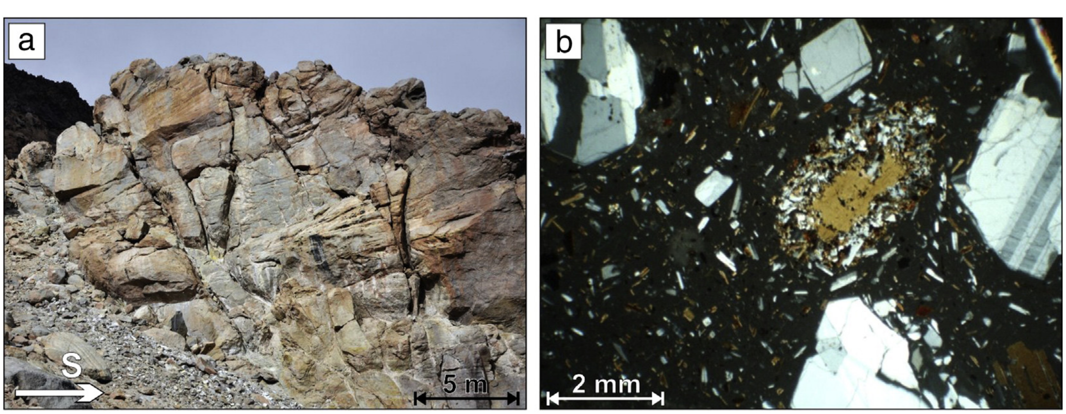

Fig. 10. *Azufre Synthem*. Field photograph (a) and thin section (b) of the lava flow in outcrop TZ13. For location see Fig. 3.

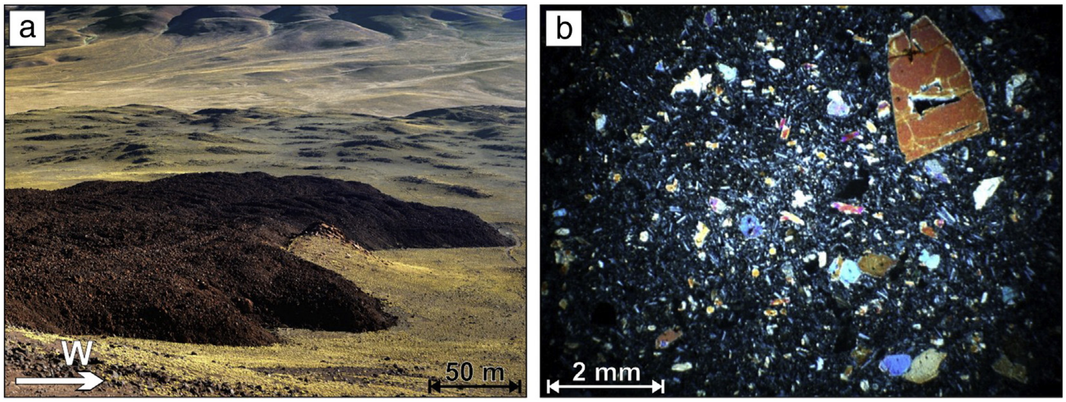

Fig. 11. *Tuzgle Synthem*. Field photograph (a) and thin section (b) of the lava flow in outcrop TZ31. For location see Fig. 3.

scattered effusive lava domes of the *Basal Dome Complex Synthem*, representing the first effusive phase in the volcano history (Figs. 4 and 6). The stratigraphic position of the *Basal Dome Complex Synthem* is coincident with the stratigraphic position of the Old Complex unit defined by Coira and Kay (1993). However, the mapped Old Complex unit (Coira and Kay, 1993) completely encloses both the Basal Dome Complex Synthem (scattered lava domes) and the following San Antonio Synthem (central volcano made of lava flows). The exact configuration of the *Basal Dome Complex Synthem* has not been defined, because it is mostly buried by the subsequent volcanic products, even if it could be partially fed along ring faults or other structures associated with the Tuzgle Ignimbrite. After this first effusive event, an unconformity marking the change from a scattered to a central feeding system has been recognized.

The building of the central volcano emplaced on top of the *Basal Dome Complex Synthem* occurred during three major effusive phases. During the first phase, the main central edifice has been emplaced, with the thick lava flows of the *San Antonio Synthem* radiating from a common source area. At the same stratigraphic level, the SAV unit, composed of a volcaniclastic deposit, has been mapped north of Cerro Tuzgle, extending up to 9 km from the volcano summit (Figs. 3 and 4). No evidences of associated pyroclastic fallout and/or pyroclastic flow deposit have been found. The stratigraphic location of the SAV deposit is coincident to that of the volcanotectonic scarp located on the northwestern flank of Cerro Tuzgle (Section 4.1). This suggests that both the SAV unit and the volcanotectonic scarp were generated during a catastrophic sector collapse of the central volcano (Fig. 6). The gravitational collapse removed the volcano summit, cutting upslope thick lava flows of the *San Antonio Synthem*, whose materials have been transported to the NNE and emplaced in a volcaniclastic fan (Fig. 9b,d). The volume of the sector collapse and resulting deposit is difficult to assess. Considering the extension of the exposed volcaniclastic fan and a mean thickness of the collapse deposit of about 20 m, an estimated volume of 0.5 km^3 should be reliable.

Despite the poor accessibility and exposure of sections of the SAV deposit, this unit presents some features that can be related to a debris flow deposit (rounded clasts and no hummocky morphology), resulting from the reworking of a more proximal debris avalanche deposit, presently completely eroded and covered by the subsequent lava flows. Similar deposits are described in numerous volcanic areas,

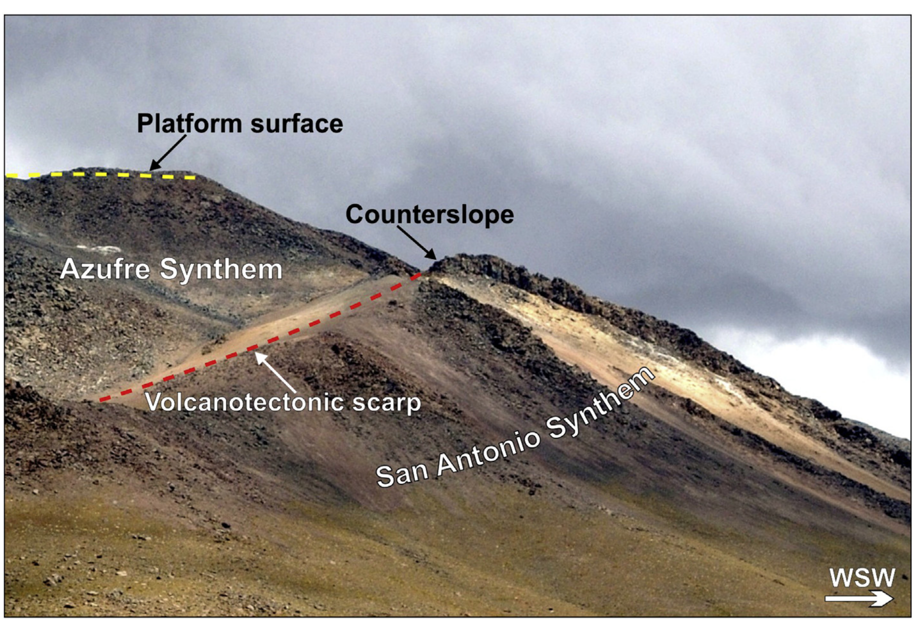

Fig. 12. Field photograph from NNW to SSE of the counterslope associated to the volcanotectonic scarp and angular unconformity at the top of the *San Antonio Synthem*. Dashed line in yellow depicts the angular unconformity named *Platform surface* at the top of the *Azufre Synthem*. (For interpretation of the references to colour in this figure legend, the reader is referred to the web version of this article.)

Fig. 13. Fault zone with white–yellow sulphur incrustations and veins in a lava flow of the Azufre Synthem in outcrop Tz42. For location see Figs. 3 and 15. (For interpretation of the references to colour in this figure legend, the reader is referred to the web version of this article.)

e.g. the Etna and the Nevado de Toluca volcanoes, where debris flows and alluvial fans are made by the sediments reworked from debris avalanche deposits originated by sector collapses (Calvari and Groppelli, 1996; Calvari et al. 1998, 2004; Capra and Macias, 2000).

The origin of this major, previously unrecognized sector failure can be attributed to a number of factors, including the regional tectonic regime, the direction of intrusion and faulting in the volcanic edifice, the local topography and a possible magmatic contribution. The Cerro Tuzgle area is tectonically characterized by a roughly E–W trending maximum horizontal stress, responsible for the orogen-parallel thrusting and the orogen-oblique strike slip faulting (e.g. Norini et al., 2013, and reference therein). This regime generated E–W eruptive fissures and faults, promoting orthogonal, N-S trending gravitational instability (e.g. Nakamura, 1977; Moriya, 1980; Siebert, 1984; Vidal and Merle, 2000) (Fig. 16). The northward dipping basement and the western and eastern lateral constraints of the orogen-parallel ranges and thrust faults probably also played a role in determining the gravitational collapse direction toward the NNE. Also, magmatic overpressure in E–W striking dikes could have played a significant role in promoting and trigger the sector failure. On the opposite side of Cerro Tuzgle, a wide morphological depression affects the southern flank of the central volcano (Fig. 16). This morphology could be the remnant of another, southward directed flank collapse, although no evidences of a corresponding volcaniclastic deposit have been identified morphologically or in outcrop.

The NNE sector collapse event and the top surface of the SAV deposit mark the unconformity at the top of the *San Antonio Synthem*. After this major gravitational collapse, the building of the central volcano resumed with the emplacement of new lava flows. These lavas have been grouped into the *Azufre Synthem*. After their emplacement, an extensive phase of hydrothermal alteration took place, with the formation of the sulphur deposits exposed in the abandoned sulphur mines on the volcano flanks (Figs. 5d, 6 and 9b). The sulphur deposits are coeval with the faults exposed on the southern flank of the volcano (Figs. 13 and 14). These hydrothermal alteration and deposition are mostly limited to the lavas of the *Azufre Synthem*, in the upper half of the volcanic cone. The constructive phase ended with the formation of a wide flat surface at the top of the volcano, whose origin can be attributed to a craterization event (Coira and Kay, 1993) or a volcanotectonic deformation, like the spreading of the highly altered hydrothermal zone of the *Azufre Synthem* (Barde-Cabusson and Merle, 2007; Merle et al., 2010) (*Platform* surface, Figs. 5a,c and 6). This surface has been used as the unconformity at the top of the *Azufre Synthem*.

The third and last constructive phase of Cerro Tuzgle was characterized by the emplacement of several extensive lava flows emitted from the volcano summit and covering its flanks and surroundings. The products of this last volcanic activity have been grouped into the *Tuzgle Synthem*, limited by the present topographic surface.

Our data suggest that both constructive and destructive phases of the volcanic evolution are consistent with the regional tectonics. No significant regional faults cut the volcanic edifice at the surface, and the structural control of the volcanic activity has been mainly exerted by the regional stress field. The E–W trending maximum horizontal stress is responsible for the direction of intrusion, faulting and gravitational instability in the volcanic edifice. The orientation of the eruptive fissures indicates that the magma has been transported to the surface throughout E–W striking hydrofractures, whose orientation is controlled by the direction of the maximum horizontal stress. The hydrothermal alteration of the volcanic edifice and the deposition of significant amounts of sulphur have been controlled by the same E–W direction, with the hydrothermal circuit established along parallel faults and hydrofractures (mineral veins). Finally, the sector collapse of the central volcano occurred toward the NNE, nearly perpendicular to the maximum horizontal stress, denoting a structural control on the gravitational instability of the volcanic edifice.

The topographic configuration of the area also played a role in the evolution of Cerro Tuzgle, with the northward dipping substrata and the buttressing of the orogen-parallel ridges partially controlling the instability of the volcanic edifice and constraining the lateral dispersion of volcaniclastic products.

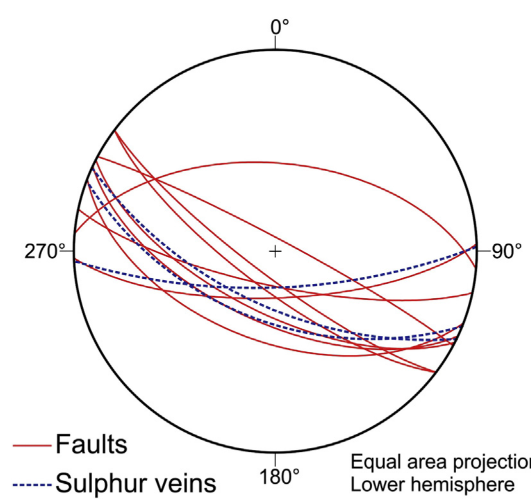

Fig. 14. Stereographic projection of faults and sulphur veins measured in outcrop Tz42. For location see Figs. 3 and 15.

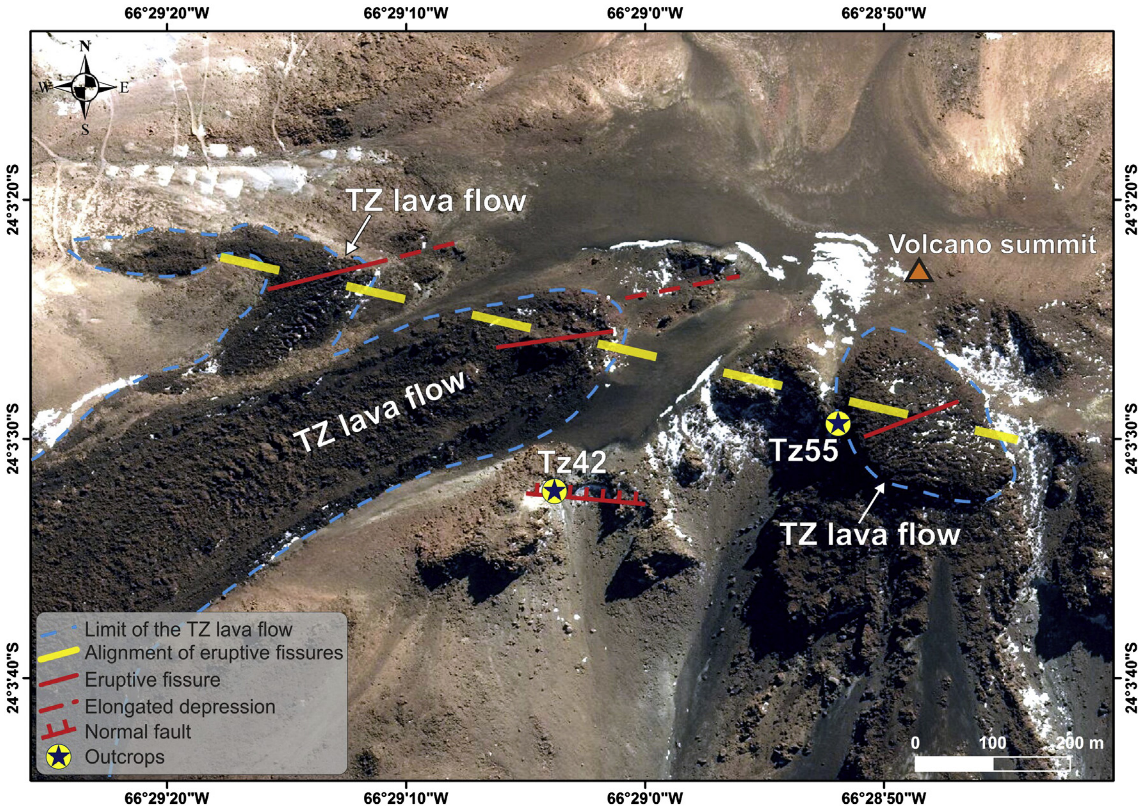

Fig. 15. Satellite view of summit area of Cerro Tuzgle. The three ENE–WSW eruptive fissures feeding the TZ lava flow and their ESE–WNW alignment are shown. Location of the outcrops Tz42 and Tz55 is also shown.

6. Concluding remarks

The principal achievements of our study can be summarized by the following points:

1. Syntemic units have been applied for the first time to a volcanic edifice of the Puna Plateau, showing the ability of this stratigraphic methodology to depict the evolution of the volcanic system in the regional geological and tectonic framework.
2. The volcanic evolution described in our work, and mainly the construction–destruction phases of the central volcano, differs considerably with respect to previous reconstructions (Coira and Kay, 1993). This could provide a new possibility to re-evaluate the evolution of the Quaternary volcanism in the Puna Plateau, including the tectonomagmatic relationships and the petrological–geochemical evolution of magmas, based on the new and accurate stratigraphic data (e.g. Coira and Kay, 1993; Acocella et al., 2011).

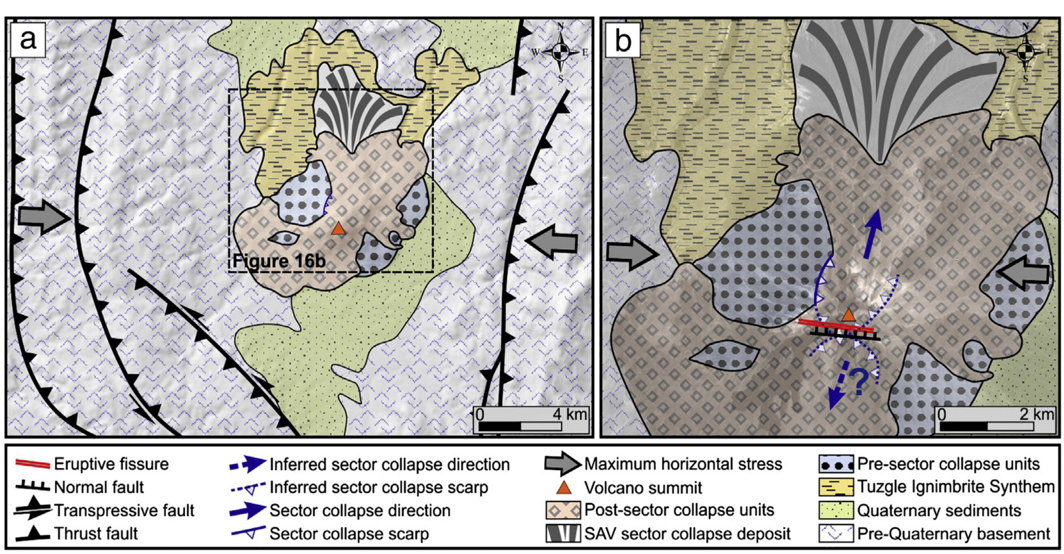

Fig. 16. Schematic geological and structural maps of the Cerro Tuzgle area (a) and of the volcanic edifice (b), showing the relationships among the flank instability, the stress regime and the topography. The *Pre-sector collapse units* include the *Basal Dome Complex Synthem* and the *San Antonio Synthem*, excluding the SAV deposit. The *Post-sector collapse units* include the *Azufre Synthem* and the *Tuzgle Synthem*. The maximum horizontal stress direction and the faults in the basement are from Norini et al. (2013). See text for explanation (Section 5).

3. A previously unreported sector collapse of Cerro Tuzgle has been recognized, and its stratigraphic position is identified. This catastrophic event is the first reported on a stratovolcano in the back-arc region of the Puna Plateau, and poses a significant concern regarding the possible occurrence of similar events in the future. Even if the region is nearly uninhabited, significant plans of mining and geothermal energy exploitation could be exposed to a non-negligible geological and volcanic hazard (e.g. Giordano et al., 2013).
4. The main non-magmatic factors controlling the Cerro Tuzgle volcanic activity have been identified. These are the regional stress regime and the topography of the substrata.
5. The integration of synthemic stratigraphy and volcanotectonic analysis at the Cerro Tuzgle stratovolcano proved to be an effective methodological approach for the study of volcanic edifices in the geological and tectonic framework of the Central Andes.

Acknowledgments

This work was supported by a CNR-Curiosity driven 2008 grant (Italy) to Gianluca Groppelli and the CONACyT CB-2009-132265 grant (Mexico) to Gianluca Norini. The Instituto Geonorte-INENCO of the Universidad de Salta-CONICET (Argentina) provided the facilities for the field campaigns. We acknowledge Maria Clara Zuluaga Velez, Guido Giordano, Numa Sousa and Massimiliano Porreca for their help in the fieldwork. We also acknowledge Lucia Capra and Olivier Merle for their valuable and constructive comments. We thank Francesco Zucca for useful discussion on the morphostructural and multispectral mapping of the Puna Plateau with ASTER and SRTM satellite data.

References

Aceñolaza, F., Aceñolaza, G., 2005. La Formacion Puncoviscana y unidades estratigraficas vinculadas en el neoproterozoico-cambrico temprano del noroeste argentine. Lat. Am. J. Sedimentol. Basin Anal. 12, 65–87.

Acocella, V., Gioncada, A., Omarini, R., Riller, U., Mazzuoli, R., Vezzoli, L., 2011. Tectonomagmatic characteristics of the back-arc portion of the Calama–Olacapato–El Toro Fault Zone, Central Andes. Tectonics 30, TC3005.

Allmendinger, R.W., Gubbels, T., 1996. Pure and simple shear plateau uplift, Altiplano–Puna, Argentina and Bolivia. Tectonophysics 259, 1–13.

Allmendinger, R.W., Ramos, V.A., Jordan, T.E., Palma, M., Isacks, B.L., 1983. Paleogeography and Andean structural geometry, northwest Argentina. Tectonics 2, 1–16.

Allmendinger, R.W., Jordan, T.E., Kay, S.M., Isacks, B.L., 1997. The evolution of the Altiplano–Puna Plateau of the Central Andes. Earth Planet. Sci. Lett. 25, 139–174.

Alonso, R., 1993. Estratigrafia del Cenozoico de la cuenca de Pastos Grandes (Puna Saltena) con enfasis en la Formacion Sijes y sus boratos. Rev. Asoc. Geol. Argent. 47 (2), 189–199.

ANCORP Working Group, 2003. Seismic imaging of a convergent continental margin and plateau in the central Andes (Andean Continental Research Project 1996—ANCORP'96). J. Geophys. Res. 108, 2328.

Aquater, 1980. Exploracion geotermica del area del Cerro Tuzgle. Provincia de Jujuy, Republica Argentina. Secretaria de Estado de Mineria, Argentina open-file report.

Assumpção, M., 1992. The regional intraplate stress field in South America. J. Geophys. Res. 97, 11,889–11,903.

Barde-Cabusson, S., Merle, O., 2007. From steep-slope volcano to flat caldera floor. Geophys. Res. Lett. 34, L10305.

Barnes, J.B., Ehlers, T.A., 2009. Endmembermodels for Andean Plateau uplift. Earth Sci. Rev. 97, 105–132.

Beck, S., Zandt, G., Myers, S.C., Wallace, T.C., Silver, P.G., Drake, L., 1996. Crustal thickness variations in the Central Andes. Geology 24, 407–410.

Bellotti, F., Capra, L., Groppelli, G., Norini, G., 2006. Tectonic evolution of the central-eastern sector of Trans Mexican Volcanic Belt and its influence on the eruptive history of the Nevado de Toluca volcano (Mexico). J. Volcanol. Geotherm. Res. (ISSN: 0377-0273) 158 (1-2), 21–36.

Blasco, G., Zappettini, E., Hongn, F., 1996. Hoja Geológica 2566-I, San Antonio de los Cobres, provincias de Salta y Jujuy, 1:250,000. ServicioGeológico Minero de Argentina, Buenos Aires, Boletín, 217.

Branca, S., Coltelli, M., Del Carlo, P., Groppelli, G., Norini, G., Pasquaré, G., 2004. Stratigraphical approaches and tools in the geological mapping of Mt. Etna Volcano. In: Pasquaré, G., Venturini, C. (Eds.), Mapping Geology in Italy, Apat – Servizio Geologico d'Italia, S.EL.CA (Firenze). ISBN: 8824025528, pp. 147–158.

Branca, S., Coltelli, M., Groppelli, G., 2011. Geological evolution of a complex basaltic stratovolcano: Mount Etna, Italy. Ital. J. Geosci. 130 (3), 306–317.

Cahill, T., Isacks, B.L., Whitman, D., Chatelain, J.L., Perez, A., Chiu, J.M., 1992. Seismicity and tectonics in Jujuy Province, northwestern Argentina. Tectonics 11, 944–959.

Calvari, S., Groppelli, G., 1996. Relevance of the Chiancone volcaniclastic deposit in the recent history of Etna Volcano (Italy). J. Volcanol. Geotherm. Res. 72 (3), 239–258.

Calvari, S., Tanner, L.H., Groppelli, G., 1998. Debris-avalanche deposits of the Milo Lahar sequence and the opening of the Valle del Bove on Etna volcano (Italy). J. Volcanol. Geotherm. Res. 87 (1), 193–209.

Calvari, S., Tanner, L.H., Groppelli, G., Norini, G., 2004. Valle del Bove, eastern flank of Etna volcano: a comprehensive model for the opening of the depression and implications for future hazards. AGU Geophys. Monogr. Ser. 143, 65–75.

Capra, L., Macias, J.L., 2000. Pleistocene cohesive debris flows at Nevado de Toluca Volcano, central Mexico. J. Volcanol. Geotherm. Res. 102, 149–167.

Carrapa, B., Adelmann, D., Hilley, G.E., Mortimer, E., Sobel, E.R., Strecker, M.R., 2005. Oligocene range uplift and development of plateau morphology in the southern central Andes. Tectonics 24 TC4011.

Coira, B., 1973. Resultados preliminares sobre la petrología del ciclo eruptivo Ordovícico concomitante con la sedimentación de la Formación Acoite en la zona de Abra Pampa, prov. de Jujuy. Rev. Asoc. Geol. Argent. 28, 85–88.

Cladouhos, I.T., Allmendinger, R.W., Coira, B., Farrar, E., 1994. Late Cenozoic deformations in the Central Andes: fault kinematics from the northern Puna, northwest Argentina and southwest Bolivia. Journal of South American Earth Sciences 7, 209–228.

Coira, B., Kay, S., 1993. Implication of Quaternary volcanism at Cerro Tuzgle for crustal and mantle evolution of the Puna Plateau, Central Andes, Argentina. Contrib. Mineral. Petrol. 113, 40–58.

Coira, B., Paris, G., 1981. Estratigrafia volcanica del area del Cerro Tuzgle (23° 50' S y 66° 45' W). Provincias del Jujuy-Salta. VIII Cong. Geol. Argen. III 659–671.

Coira, B.L., Davidson, J.D., Mpodozis, C., Ramos, V.A., 1982. Tectonic and magmatic evolution of the Andes of northern Argentina and Chile. Earth Sci. Rev. 18, 303–332.

Coutand, I., Cobbold, P.R., de Urreiztieta, M., Gautier, P., Chauvin, A., Gapais, D., Rossello, E. A., López Gamundí, O., 2001. Style and history of Andean deformation, Puna plateau, northwestern Argentina. Tectonics 20, 210–234.

Coutand, I., Carrapa, B., Deeken, A., Schmitt, A.K., Sobel, E.R., Strecker, M.R., 2006. Propagation of orogenic barriers along an active range front: insights from sandstone petrography and detrital apatite fission-track thermochronology in the intramontane Angastaco basin. NW Argentina. Basin Research 18, 1–26.

de Silva, S.L., Francis, P.W., 1991. Volcanoes of the Central Andes. Springer-Verlag, New York (213 pp.).

de Urreiztieta, M., Gapais, D., Le Corre, C., Cobbold, P.R., Rossello, E., 1996. Cenozoic dextral transpression and basin development at the southern edge of the Puna Plateau, northwestern Argentina. Tectonophysics 254, 17–39.

DeMets, C., Gordon, R.G., Vogt, P., 1994. Location of the Africa–Australia–India triple junction and motion between the Australian and Indian plates: results from an aeromagnetic investigation of the Central Indian and Carlsberg ridges. Geophys. J. Int. 119, 893–930.

Dewey, J.F., Lamb, S.H., 1992. Active tectonics of the Andes. Tectonophysics 205, 79–95.

Elger, K., Oncken, O., Glodny, J., 2005. Plateau-style accumulation of deformation: Southern Altiplano. Tectonics 24, TC4020.

Fink, J.H., Pollard, D.D., 1983. Structural evidence for dikes beneath silicic domes, Medicine Lake Highland Volcano, California. Geology 11, 458–461.

Galliski, M.A., Viramonte, J.G., 1988. The Cretaceous paleorift in northwestern Argentina: a petrologic approach. J. S. Am. Earth Sci. 1, 329–342.

Giordano, G., Pinton, A., Cianfarra, P., Baez, W., Chiodi, A., Viramonte, J., Norini, G., Groppelli, G., 2013. Structural control on geothermal circulation in the Cerro Tuzgle–Tocomar geothermal volcanic area (Puna plateau, Argentina). J. Volcanol. Geotherm. Res. 249, 77–94.

González-Ferrán, O., 1995. Volcanes de Chile. Instituto Geografico Militar, Santiago. Chile (640 pp.).

Gripp, A., Gordon, R., 1990. Current velocities relative to the hotspots incorporating the NUVEL-1 global plate motion model. Geophys. Res. Lett. 17, 1109–1112.

Guzmán, S.R., Petrinovic, I.A., Brod, J.A., 2006. Pleistocene mafic volcanoes in the Puna-Cordillera Oriental boundary, NW-Argentina. J. Volcanol. Geotherm. Res. 158, 51–69.

Hongn, F., Del Papa, C., Powell, J., Petrinovic, I., Mon, R., Deraco, V., 2007. Middle Eocene deformation and sedimentation in the Puna-Eastern Cordillera transition (23-26S): control by preexisting heterogeneities on the pattern of initial Andean shortening. Geology 35, 271–274.

Isacks, B.L., 1988. Uplift of the Central Andean Plateau and bending of the Bolivian Orocline. J. Geophys. Res. 93, 3211–3231.

Jordan, T.E., Isacks, B.L., Allmendinger, R.W., Brewer, J.A., Ramos, V.A., Ando, C.J., 1983. Andean tectonics related to geometry of subducted Nazca plate. GSA Bull. 94, 341–361.

Kay, S.M., Coira, B.L., 2009. Shallowing and steepening subduction zones, continental lithospheric loss, magmatism, and crustal flow under the Central Andean Altiplano–Puna Plateau. In: Kay, S.M. (Ed.), Backbone of the Americas: shallow subduction, plateau uplift, and ridge and terrane collision. Geological Society of America Memoir. 204, pp. 229–259.

Kay, S.M., Coira, B.L., Caffe, P.J., Chen, C.H., 2010. Regional chemical diversity, crustal and mantle sources and evolution of central Andean Puna plateau ignimbrites. J. Volcanol. Geotherm. Res. 198, 81–111.

Kley, J., Monaldi, C.R., 1998. Tectonic shortening and crustal thickness in the Central Andes: how good is the correlation? Geology 26, 723–726.

Kley, J., Monaldi, C.R., 2002. Tectonic inversion in the Santa Barbara System of the central Andean foreland thrust belt, northwestern Argentina. Tectonics 21 (6), 1061. http://dx.doi.org/10.1029/2002TC902003.

Klotz, J., Angermann, D., Michel, G.W., Porth, R., Reigber, C., Reinking, J., Viramonte, J., Perdomo, R., Rios, V.H., Barrientos, S., Barriga, R., Cifuentes, O., 1999. GPS-derived deformation of the central Andes including the 1995 Antofagasta Mw = 8.0 earthquake. Pure Appl. Geophys. 154, 709–730.

Koukharsky, M., Munizga, F., 1990. Los volcanes Guanaquero, Chivinar, Tul Tul, del medio y Pocitos, Provincia de Salta. Litologia y edades K/Ar. Actas del Congreso Geologico Argentino, San Juan, Buenos Aires, Asociacion Geologica Argentina. 1, pp. 54–57.

Kraemer, B., Adelmann, D., Alten, M., Schnurr, W., Erpenstein, K., Kiefer, E., van den Bogaard, P., Görler, K., 1999. Incorporation of the Paleogene foreland into the Neogene Puna plateau: the Salar de Antofalla area. NW Argentina. Journal of South American Earth Sciences 12, 157–182.
Marrett, R.A., Strecker, M.R., 2000. Response of intracontinental deformation in the Central Andes to the late Cenozoic reorganization of South American Platemotions. Tectonics 19, 452–467.
Marrett, R.A., Allmendinger, R.W., Alonso, R.N., Drake, R.E., 1994. Late Cenozoic tectonic evolution of the Puna Plateau and adjacent foreland, northwestern Argentine Andes. Journal of South American Earth Sciences 7, 179–207.
Marquillas, R.A., del Papa, C., Sabino, I.F., 2005. Sedimentary aspects and paleoenvironmental evolution of a rift basin: Salta Group (Cretaceous–Paleogene), northwestern Argentina. Int. J. Earth Sci. (Geol. Rundsch.) 94, 94–113.
Matteini, M., Mazzuoli, R., Omarini, R., Cas, R., Maas, R., 2002. Geodynamical evolution of the central Andes at 24°S as inferred by magma composition along the Calama–Olocapato–El Toro transversal volcanic belt. J. Volcanol. Geotherm. Res. 118, 225–228.
Mazzuoli, R., Vezzoli, L., Omarini, R., Acocella, V., Gioncada, A., Matteini, M., Dini, A., Guillou, H., Hauser, N., Uttini, A., Scaillet, S., 2008. Miocene magmatism and tectonics of the easternmost sector of the Calama–Olacapato–El Toro fault system in Central Andes at 24°S: insights into the evolution of the Eastern Cordillera. Geol. Soc. Am. Bull. 120, 1493–1517.
Mendez, V., Navarini, N., Plaza, D., Viera, O., 1973. Faja Eruptiva de la Puna Oriental. V Congreso geológico Argentino Actas. 4, pp. 89–100.
Merle, O., van Wyk de Vries, B., Barde-Cabusson, S., 2010. Hydrothermal calderas. Bull. Volcanol. 72, 131–147.
Mon, R., 1987. Structural geology of two geothermal area in the Andes: Copahue and Tuzgle (Argentina). Bulletin of the International Association of Engineering Geology 35, 79–85.
Monaldi, C.R., Salfity, J.A., Kley, J., 2008. Preserved extensional structures in an inverted Cretaceous rift basin, northwestern Argentina: outcrop examples and implications for fault reactivation. Tectonics 27, TC1011.
Moriya, I., 1980. "Bandaian Eruption" and landforms associated with it. Collection of articles in memory of retirement of Prof. K. Nishimura from Tohoku Univ. pp. 214–219.
Nakamura, K., 1977. Volcanoes as possible indicators of tectonic stress. J. Volcanol. Geotherm. Res. 2, 1–16.
Norabuena, E., Dixon, T.H., Stein, S., Harrison, C.G.A., 1999. Decelerating Nazca-South America and Nazca-Pacific plate motions. Geophys. Res. Lett. 26, 3405–3408.
Norini, G., Groppelli, G., Lagmay, A.M.F., Capra, L., 2006. Recent left-oblique slip faulting in the eastern-central Trans-Mexican Volcanic Belt. Seismic hazard and geodynamic implications. Tectonics (ISSN: 0278-7407) 25, 1–21 (TC4012).
Norini, G., Capra, L., Groppelli, G., Agliardi, F., Pola, A., Cortes, A., 2010. Structural architecture of the Colima Volcanic Complex. J. Geophys. Res. Solid Earth (ISSN: 0148-0227) 115, 1–20 (B12209).
Norini, G., Baez, W., Becchio, R., Viramonte, J., Giordano, G., Arnosio, M., Pinton, A., Groppelli, G., 2013. The Calama–Olacapato–El Toro Fault System in the Puna Plateau, Central Andes: geodynamic implications and stratovolcanoes emplacement. Tectonophysics 608, 1280–1297.
Omarini, R., Sureda, R., Götze, H., Seilacher, A., Pflüger, F., 2001. Puncoviscana folded belt in northwestern Argentina: testimony of Late Proterozoic Rodinia fragmentation and pre-Gondwana collisional episodes: a reply. International Journal of Earth Sciences 90, 894–902.
Palma, R.M., 2000. Lacustrine facies in the Upper Cretaceous Balbuena subgroup (Salta Group): Andina Basin, Argentina. In: Gierlowski- Kordesch, E.H., Kelts, K.R. (Eds.), Lake basins through space and time: AAPG Studies in Geology. 46, pp. 323–328.
Pasquaré, F.A., Tibaldi, A., 2003. Do transcurrent faults guide volcano growth? The case of NW Bicol Volcanic Arc, Luzon, Philippines. Terra Nova 15, 204–212.
Petrinovic, I.A., Riller, U., Brod, A., 2005. The Negra Muerta volcanic complex, southern Central Andes: geochemical characteristics and magmatic evolution of an episodic volcanic centre. J. Volcanol. Geotherm. Res. 140, 295–320.
Petrinovic, I.A., Riller, U., Alvarado, G., Brod, J.A., Arnosio, M., 2006. Bimodal volcanism in a tectonic transfer zone: evidence for tectonically controlled magmatism in the southern Central Andes, NW Argentina. J. Volcanol. Geotherm. Res. 152, 240–252.
Petrinovic, I.A., Martí, J., Aguirre-Díaz, G.J., Guzmán, S., Geyer, A., Salado Paz, N., 2010. The Cerro Águas Calientes caldera, NW Argentina: an example of a tectonically controlled, polygenetic collapse caldera, and its regional significance. J. Volcanol. Geotherm. Res. 194, 15–26.
Pieri, D., Abrams, M., 2004. ASTER watches the world's volcanoes: a new paradigm for volcanological observations from orbit. Journal of Volcanology and Geothermal Research 135, 13–28.
Ramelow, J., Riller, U., Romer, R.L., Oncken, O., 2006. Kinematic link between episodic trapdoor collapse of the Negra Muerta Caldera and motion on the Olacapato–El Toro Fault Zone, southern central Andes. Int. J. Earth Sci. 95, 529–541.
Ramos, V.A., 2009. Anatomy and global context of the Andes: main geologic features and the Andean orogenic cycle. In: Kay, S.M., Ramos, V.A., Dickinson, W.R. (Eds.), Backbone of the Americas: shallow subduction, plateau uplift, and ridge and terrane collision. Geological Society of America Memoir. 204, pp. 31–65.
Reyes, F.C., Salfity, J.A., 1973. Cosideraciones sobre la estratigrafia del Cretácico (Subgrupo Pirgua) del Noeste Argentino. Actas del Congreso Geologico Argentino, San Juan, Buenos Aires, Asociacion Geologica Argentina. 3, pp. 355–385.
Reynolds, J., Galli, C., Hernandez, R., Idleman, B., Kotila, J.M., Hilliard, R.V., Naeser, C.W., 2000. Middle Miocene tectonic development of the transition zone, Salta Province, northwest Argentina: magnetic stratigraphy from the Meta´n Subgroup, Sierra de Gonza´lez. Geol. Soc. Am. Bull. 112, 1736–1751.
Riller, U., Oncken, O., 2003. Growth of the central Andean Plateau by tectonic segmentation is controlled by the gradient in crustal shortening. J. Geol. 111, 367–384.
Riller, U., Petrinovic, I., Ramelow, J., Strecker, M.R., Onken, O., 2001. Late Cenozoic tectonism, collapse caldera and plateau formation in the Central Andes. Earth Planet. Sci. Lett. 188, 299–311.
Sainato, C.M., Pomposiello, M.C., 1997. Two-dimensional Magnetotelluric and Gravity Models of the Tuzgle Volcano Zone (Jujuy Province, Argentina). Journal of South American Earth Sciences 10, 247–261.
Salfity, J.A., 1985. Lineamentos transversales al rumbo andino en el noroeste argentino. Actas IV Congreso Geológico Chileno. 2. Asoc. Geol. Argentina, Antofagasta, Chile pp. 119–137.
Salfity, J.A., Marquillas, R.A., 1994. Tectonic and sedimentary evolution of the Cretaceous-Eocene Salta Group basin, Argentina. In: Salfity, J.A. (Ed.), Cretaceous Tectonics of the Andes. Vieweg Verlag, Wiesbaden, Germany, pp. 266–315.
Salfity, J.A., Monaldi, C.R., 2006. Hoja Geológica 2566-IV: Metán (1:250,000). Programa Nacional de Cartas Geológicas de la República Argentina, boletin, 319, Buenos Aires, 80 pp.
Salfity, J.A., Monaldi, C.R., Marquillas, R.A., Gonzalez, R.E., 1993. La inversion tectonica del Umbral de Los Gallos en la cuenca del Grupo Salta durante la Fase Incaica. paper presented at 12th Congreso Geolo´gico Argentino and 2nd Congreso Nacional de la Exploracion Hidrocarburos, Asociacion Geol. Argentina and Inst. Argentino del Petroleo y del Gas, Mendoza, Argentina.
Sanchez, M.C., Salfity, J.A., 1999. La cuenca cámbrica del Grupo Mesón en el Noroeste Argentino: desarrollo estratigráfico y paleogeográfico. Acta Geol. Hisp. 34 (2–3), 123–139.
Schwab, K., Lippolt, H., 1976. K–Ar mineral ages and late Cenozoic history of the Salar Cauchari area (Argentina, Puna). In: Gonzales-Ferran, O. (Ed.), Proceedings of the Symposium on Andean and Antarctic Volcanological Problems: Santiago. International Association of the Volcanology and Chemistry of the Earth's Interior Special Series, pp. 698–714.
Siebert, L., 1984. Large volcanic debris avalanches: characteristics of source areas, deposits, and associated eruptions. J. Volcanol. Geotherm. Res. 22, 163–197.
Sobel, E.R., Hilley, G.E., Strecker, M.R., 2003. Formation of internally drained contractional basins by aridity-limited bedrock incision. Journal of Geophysical Research 108, 2344.
Stern, C.R., 2004. Active Andean volcanism: its geologic and tectonic setting. Rev. Geol. Chile 31 (2), 161–206.
Tibaldi, A., 1995. Morphology of pyroclastic cones and tectonics. J. Geophys. Res. 100 (B12), 24,521–24,535.
Trumbull, R.B., Riller, U., Oncken, O., Scheuber, U.E., Munier, K., Hongn, F., 2006. The timespace distribution of Cenozoic volcanismin the south-central Andes: a newdata compilation and some tectonic implications. In: Oncken, O., et al. (Eds.), The Andes: active subduction orogenyFrontiers Earth Science. 1. Springer, New York, pp. 29–43.
Turner, 1960. Estratigrafía de la Sierra de Santa Victoria y adyacencias. Bol. Acad. Nac. Cienc. Repub. Argent. 41 (2), 163–196.
Turner, J.C.M., 1964. Descripción de la Hoja Geológica 7c, Nevado de Cachi, Salta. Boletín. Dirección Nacional de Geología y Minería. 99.
USGS, 2006. Shuttle Radar Topography Mission, 3 Arc Second scenes, Global Land Cover Facility. University of Maryland, College Park, Maryland.
Vidal, N., Merle, O., 2000. Reactivation of basement faults beneath volcanoes: a new model of flank collapse. J. Volcanol. Geotherm. Res. 99, 9–26.
Viramonte, J.G., Petrinovic, I.A., 1990. Cryptic and partially buried calderas along a strike-slip fault system. In: Inst. Français de Rech. Sci (Ed.), the Central Andes, ISAG Grenoble. Ed. De l'Orstom, Paris, pp. 317–320.
Viramonte, J.G., Omarini, R.H., Araña Saavedra, V., Aparicio, A., Garcia Cacho, L., 1984. Edad génesis y mecanismos de erupción de las riolítas granatíferas de San Antonio de Los Cobres, provincia de Salta. IX Congreso Geológico Argentino. 3. Asoc. Geol. Argentina, Bariloche, Argentina, pp. 216–233.
Viramonte, J.G., Kay, S.M., Becchio, R., Escayola, M., Novitski, I., 1999. Cretaceous rift related magmatism in Central-western South America. J. South Am. Earth Sci. 12, 109–121.
Viramonte, J.M., Becchio, R., Viramonte, J.G., Pimentel, M., Martino, R., 2007. Ordovician Igneous and metamorphic units in the southern Puna: new U/Pb and Sm/Nd data and implications for the evolution of NW Argentina. J. S. Am. Earth Sci. 24, 167–183.
Wigger, P., Schmitz, M., Araneda, M., Asch, G., Baldzuhn, S., Giese, P., Heinsohn, W.D., Martlnez, E., Ricaldi, E., Rower, P., Viramonte, J., 1994. Variation in the crustal structure of the southern Central Andes deduced from seismic refraction investigations. In: Reutter, K.J., Scheuber, E., Wigger, P.J. (Eds.), Tectonics of the Southern Central Andes: Structure and Evolution of an Active Continental Margin. Springer-Verlag, Berlin, pp. 23–48.
Yuan, X., Sobolev, S.V., Kind, R., Oncken, O., Bock, G., Asch, G., Schurr, B., Graeber, F., Rudlol, A., Hanka, W., Wylegalla, K., Tibi, R., Haberland, C.H., Rietbrock, A., Giese, P., Wigger, P., Rower, P., Zandt, G., Beck, S., Wallace, T., Pardo, M., Comte, D., 2000. Subduction and collision processes in the Central Andes constrained by converted seismic phases. Nature 408, 958–961.
Zang, A., Stephansson, O., 2010. Stress Field of the Earth's Crust. Springer Science + Business Media, (322 pp.).